Journal of the European Ceramic Society 20 (2000) 2275–2295

Progress in SiAlON ceramics

V.A. Izhevskiy [a,1], L.A. Genova [a], J.C. Bressiani [a], F. Aldinger [b,*]

[a] *Instituto de Pesquisas Energéticas e Nucleares, IPEN/CNEN-SP, Trav. R, 400, Cidade Universitária, São Paulo, SP-05508-900, Brazil*
[b] *Max-Planck-Institut für Metallforschung und Universität Stuttgart, Institut für Nichtmetallische Anorganische Materialien, Heisenbergstrasse 5, D-70569, Stuttgart, Germany*

Received 9 June 1999; received in revised form 21 December 1999; accepted 30 January 2000

Abstract

In view of the considerable progress that has been made over the last several years on the fundamental understanding of phase relationships, microstructural design, and tailoring of properties for specific applications of rare-earth doped SiAlONs, a clear review of current understanding of the basic regularities lying behind the processes that take place during sintering of SiAlONs is timely. Alternative secondary phase development, mechanism and full reversibility of the α′ to β′ transformation in relation with the phase assemblage evolution are elucidated. Reaction sintering of multicomponent SiAlONs is considered with regard of wetting behavior of silicate liquid phases formed on heating. Regularities of SiAlON's behavior and stability are tentatively explained in terms of RE element ionic radii and acid/base reaction principle.

Keywords: Phase equilibria; Phase transformations; SiAlONs; Sintering

Contents

* Corresponding author.
E-mail address: aldinger@aldix.mpi-stuttgart.mpg.de (F. Aldinger).
[1] Invited scientist, on leave from the Institute for Problems of Material Science, National Academy of Sciences of Ukraine, Kiev, Ukraine.

0955-2219/00/$ - see front matter
PII: S0955-2219(00)00039-X

1. Introduction

SiAlONs is a general name for a large family of the so-called ceramic alloys based on silicon nitride. Initially, they were discovered in the early 1970s[1–3] and have been developed actively since. In the following years, fully dense polycrystalline bodies were prepared by pressureless sintering techniques. Profound understanding of basic regularities of the interrelation between the starting powder's properties, processing parameters and the properties of consolidated materials was achieved. The majority of the SiAlON phases were investigated and characterized. The latter applies to β-SiAlON, α-SiAlON, AlN polytypoid phases, O′-SiAlON, as well as to a variety of crystalline secondary phases, mostly silicates, alumosilicates, and oxynitrides. Nitrogen-rich glasses were also thoroughly investigated. The vast amount of data accumulated was critically evaluated and summarized in several reviews.[4–6] Although the initial goal of creating a single-phase silicon nitride-based ceramics without any intergranular amorphous phases due to the transient liquid phase sintering was not achieved, SiAlON ceramics became one of the commercially produced high-tech ceramic materials.

There are two SiAlON phases that are of interest as engineering ceramics, α-SiAlON and β-SiAlON, which are solid solutions based on α and β-Si_3N_4 structural modifications, respectively, and designated respectively as α′ and β′. β-SiAlON is formed by simultaneous equivalent substitution of Al–O for Si–N and has most commonly been described by the formula $Si_{6-z}Al_zO_zN_{8-z}$. In this formula z can be varied continuously from zero to about 4.2.[7–9] The homogeneity region of β-SiAlON extends along the Si_3N_4–(Al_2O_3AlN) tie line of the phase diagram. The unit cell of β′ contains two Si_3N_4 units. The α-SiAlON has a unit cell comprising four Si_3N_4 units and forms a limited two-dimensional phase region in the plane $Si_3N_4\frac{4}{3}(Al_2O_3\cdot AlN) - MeN\cdot 3AlN$ of the Me–Si–Al–O–N phase diagram. In the latter diagram the β-SiAlON falls on one border of the plane mentioned. Of special interest are the Me–Si–Al–O–N systems where the α-SiAlON phase is stabilized by Me ions, such as lithium, magnesium, calcium, yttrium, and the rare-earth (RE) metals except lanthanum, cerium, praseodymium, and europium.[10–12] The homogeneity range composition of α-SiAlON can be described by the general formula $Me_mSi_{12-(pm+n)}Al_{(pm+n)}O_nN_{16-n}$ for a metal ion Me^{p+}. Two substitution mechanisms may act; the first is similar to that of β-SiAlON with n (Si + N) being replaced by n (Al + O). The second mechanism is further replacement of $pmSi^{4+}$ by $pmAl^{3+}$, the electron balance being retained by incorporation of mMe^{p+} into the phase structure.

The α-SiAlON phase region was most extensively studied in the Y–Si–Al–O–N system, where the two-dimensional phase field extension can be expressed as $Y_xSi_{3-(3x+n)}$-$Al_{(3x+n)}O_nN_{4-n}$, with $0.08 < x < 0.17$ and $0.13 < n < 0.31$.[11,13–16] The lower solubility limit is located at $x \approx 0.08$ and 0.20 for cations with the radius of 0.095 to 0.1 nm, and significantly higher, $x = 0.25$, for small cations such as ytterbium with a radius of ≈ 0.085 nm.[17] More recent investigations,[18,19] showed that the α phase area becomes larger with the decreasing size of the Me ion, i.e. in the order Nd (0.99Å) < Sm (0.96Å) < Dy (0.91Å) < Y(0.89Å) < Yb(0.87Å). Moreover, the Yb system has been shown to have the largest α-SiAlON phase area because both Yb^{3+} and Yb^{2+} ions are present in the α-SiAlON phase. The exact amount of Yb^{2+} ions present has not been determined but is anyhow expected to vary with the temperature and preparation conditions used.The n value of the Yb-α-SiAlON phase has been shown to increase with increasing Yb^{2+} content, and m to decrease, implying that the most oxygen-rich α-SiAlON phase will be found in the Yb-α-SiAlON system.

By changing the overall composition in the Y-SiAlON system, (α + β)-SiAlON ceramics can be prepared with a varying α-SiAlON:β-SiAlON phase ratio.[20, 21] α-SiAlON phase normally appears as equiaxed grains in the microstructure of the material, while β-SiAlON phase forms elongated grains with an aspect ratio of 4 to 10. However, some recent research of, in particular, Sm- and Y-doped α-SiAlONs,[22, 23] which provides even better possibilities of microstructure tailoring. It is evident from its chemical composition that α-SiAlON phase offers possibility of reducing the amount of residual glassy grain-boundary phase by incorporating constituents of sintering aids into the crystal structure, which otherwise will be present as substantial amounts of residual glassy phase and deteriorate the high temperature performance of the material. Thus, in principle, α-SiAlON enables the preparation of the practically glass-free SiAlON composites, which may become interesting candidates for high-temperature structural and engineering applications.

The possibility of varying the α-SiAlON:β-SiAlON phase ratio by slightly changing the overall composition was shown to open many possibilities to prepare Y-SiAlON ceramics with desired properties. This is of the utmost importance in connection with tailoring the properties for specific applications. Hardness increases markedly with increasing α-SiAlON phase content, whereas the fracture toughness decreases. High α-SiAlON content also improves oxidation resistance of the material and the thermal shock resistance.[4] Other ways of changing properties of SiAlON ceramics by means of replacing Y_2O_3 by other RE-oxide additives were also investigated.[24] Precisely this direction of research lead to discovery of the full reversibility of the α′ to β′ transformation for certain phase assemblies under conditions of post-sintering heat treatment.[25–27] It has been observed that the α-SiAlON phase is less stable at low temperatures and decomposes into rare-

earth-rich intergranular phase(s) and β-SiAlON with a remarkably elongated crystal morphology. The extent of the transformation is more pronounced with increased heat-treatment temperature. The mechanism of the fully reversible α′ to β′ transformation was investigated by the same authors.[28] This transformation provides an excellent possibility for optimizing phase content and microstructure without further additions of oxides and nitrides merely by heat treatment at appropriately chosen temperatures. In this way, premeditated values of hardness, strength and toughness can be achieved from a single starting composition, which opens new perspectives for their successful application.

The objective of the present review, therefore, is to provide a comprehensive overall view of the new developments in SiAlONs that will facilitate advances of this subject, and allow areas for further study to be more clearly identified. The review will cover such important issues as thermal stability of different RE-doped (α + β) SiAlON composites, phase relationships in this systems, alternative secondary phases for SiAlON ceramics, and mechanisms of reversible α′ to β′ transformation.

2. Occurrence of nitrogen melilite and nitrogen woehlerite solid solutions containing aluminum

Nitrogen-containing (or N-)melilites and nitrogen-containing (or N-) woehlerites (N-woehlerites are also known as J-phases) have been recently closely re-evaluated as the candidates for alternative secondary phases in Si_3N_4-based ceramics after the Al-containing solid solutions of this phases were discovered and investigated.[29–32] Both phases were discovered relatively early in the course of silicon nitride development and at the time were considered as undesirable secondary phases due to their poor oxidation resistance at temperature between 900 and 1100°C.[33] Under such conditions they oxidize rapidly to crystobalite and *y*-$R_2Si_2O_7$ (where R = yttrium or rare earth metal) with a ~30% increase in specific volume, and this results in catastrophic cracking and total failure of material. N-melilites have the general formula $R_2Si_3O_3N_4$ and occur as an intermediate phase during sintering of a number of Si_3N_4-based ceramics. In particular, N-melilite is located in the phase compatibility regions of α−(α + β)-SiAlONs, which in theory can produce a good microstructure of SiAlONs N-melilite as the only secondary phase. N-melilite [M(R)], has a tetragonal structure that is built up of an infinite linkage of corner-sharing $Si(O,N)_4$ units in tetrahedral sheets perpendicular to the [001] direction. Sandwiched between these sheets are Y^{3+} or rare earth Ln^{3+} ions which hold the silicon oxynitride layers together.[34] The structure of N-woehlerite is monoclinic and contains either $Si_2O_5N_2$ or Si_2O_6N ditetrahedral units containing N in the bridging position and arranged lengthwise along the a-axis. These units are linked by RE polyhedra.

Both types of phases are very stable refractory compounds and occur in almost all rare-earth SiAlON systems.[34] With high melting points (~1900°C for yttrium N-melilite[35]) and a composition close to a nitrogen-rich limit of the liquid region, these phases fulfill some of the ideal requirements for a grain boundary phase in SiAlON ceramics. However, the most important distinction of melilite–woehlerite type of secondary phases is that they do not form a eutectic with the matrix Si_3N_4 while the traditional oxide-base secondary phases form one unconditionally. This becomes absolutely obvious if one considers phase diagrams of R–Si–(Al/O)–N systems. A liquid phase region exists at high temperature on all these diagrams, separating the Si_3N_4 corner and the plane of additive oxides and their compounds. In contrast, there is no liquid phase region between M(R)/J(R) and Si_3N_4 corner on any of the phase diagrams of R–Si–(Al/O)–N systems. Although some liquid does form during initial heating because of the ternary eutectic of SiO_2, Al_2O_3, and R_2O_3, the liquid should be consumed largely by Si_3N_4 to form M(R) or J(R). Thus, sintering of the latter compositions is relatively difficult at the intermediate temperature for lack of liquid, but it improves drastically once the melting point of M(R) and J(R) is exceeded. Indeed, the lack of liquid at the intermediate temperature could be advantageous because it reduces the possibility of melt evaporation and massive powder relocation. Additionally, both melilite and woehlerite type phases crystallize readily on cooling directly from the liquid, which leads to quicker and much more complete crystallization as compared to any devitrification process. The latter occurs in solid state, and consequently all diffusion processes are by several orders of magnitude slower than in the liquid.

The catastrophic oxidation at intermediate temperatures mentioned above can be avoided by formation in the material of melilite and woehlerite based solid solutions containing aluminum instead of pure M(R) and J(R). The general formulas of these solid solutions are $R_2Si_{3-x}Al_xO_{3+x}N_{4-x}$ and $R_4Si_{2-x}Al_xO_{7+x}N_{2-x}$, respectively. The solid solutions will be further referred to as M′(R) and J′(R). In these phases, Si–N bonds are progressively being replaced by Al–O bonds, leading to the increase of the oxygen content, which in turn improves the oxidation resistance.

Until now, the regularities of solid solubility of aluminum in M(R) and J(R) were studied for the majority of RE elements (Nd, Sm, Gd, Dy, Yb, and Y) that are used in SiAlON production. It was unequivocally shown that the solid solubility range of M′(R) phases in respect of aluminum are determined by ionic radius of the RE element. With decreasing ionic radius the solubility limits in melilite solid solution decrease. For elements with large ionic radii, i.e., R = Nd and Sm, up to one Si

Table 1
Compilation of experimental data on the formation of N-melilite in different systems[40]

Cation	Ionic radius r_R^{3+}(Å)[a]	$r_R^{3+}:r_O^{2-}$	Al-free N-melilite formation	Formation of M′(R)	Maximum aluminum solubility in M′(R)
La^{3+}	1.016	0.77	Does not form	No study	Experimental data currently unavailable
Nd^{3+}	0.995	0.75	Observed	Observed	$x = \sim 1.0$
Sm^{3+}	0.964	0.73	Observed	Observed	$x = \sim 1.0$
Dy^{3+}	0.908	0.69	Observed	Observed	$x = \sim 0.7$
Y^{3+}	0.893	0.68	Observed (not at 1500°C)	Observed	$x = \sim 0.7$
Yb^{3+}	0.858	0.65	Does not form	No study	Experimental data currently unavailable

can be replaced by Al. Consequently, yttrium melilite has the lowest observed aluminum solubility ($x = 0.6$) in rare earth elements melilite solid solutions.[36] Both ytterbium and lanthanum do not stabilize N-melilite.[37–39] It was, however, shown that ytterbium forms J′(R) solid solution that can serve as an alternative secondary phase in this system. On the other hand, lanthanum forms only the M′ phase with the highest substitution level ($x = 1$), which is a point phase in La–Si–Al–O–N system, and the M′(La) homogeneity range does not exist. Here it must be specifically emphasized that phase pure M(R) or M′(R) were never formed neither in the form of a secondary phase in any RE-doped SiAlON system, nor if synthesized separately according to stoichiometry. Appreciable amounts of J′(R), REAG ($RE_3Al_5O_{12}$) or other phases were present depending on the RE oxide used, the amount of J′(R) increasing with the decrease of the RE ionic radius. The results of the M′(R) solubility range determination for different systems are summarized in Table 1.[40]

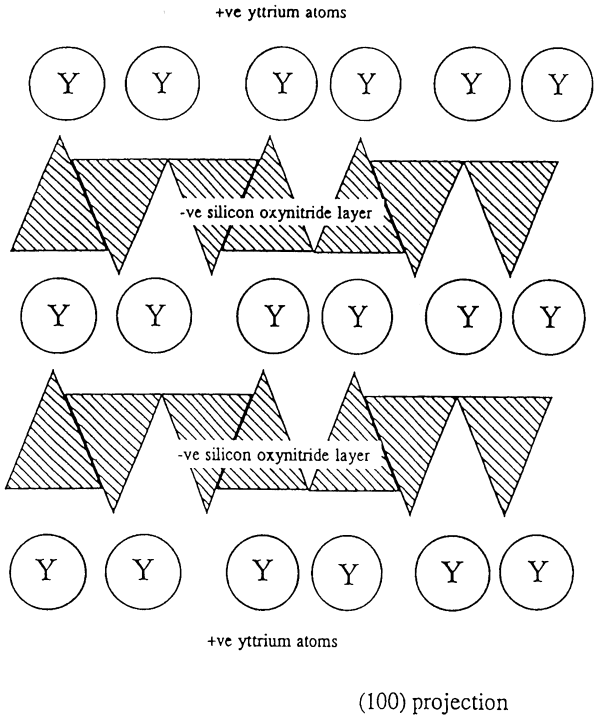

Fig. 1. Schematic representation of the structure of yttrium N-melilite showing separation of the negatively charged silicon oxynitride layers by Y^{3+} cations.[40]

The data on the correlation between the x value in M′(R) solid solution formula and the lattice parameters of M′(R) were determined for the majority of RE stabilizing elements.[29,36,41] Linear increase of the lattice parameters with increasing of the x values was observed for all systems investigated up to a certain x value for respective M′(R) phases. However, these x values do not necessarily represent true solubility limits as all samples contained additional phases, as it was mentioned earlier, some of which were rare earth rich. It can, however, be noted that the c/a ratios are almost constant with increasing x-value for each M′(R) phase which indicates that the structural changes introduced when Si–N pairs are replaced by Al–O ones are isotropic in all M′(R) phases studied.

Since the nominal x value, i.e., the one determined by the powder mixture composition, was not relevant due to the multiphase nature of the synthesized materials, SEM–EDS studies have been used to estimate solubility limits of Al in various M′(R) phases. The maximum aluminum content, as determined in Ref. 36, were $x = 0.98$, 0.9, 0.78, 0.71, and 0.57 for R = Nd, Sm, Gd, Dy, and Y, respectively. Thus, in M′(Nd) and M′(Sm) systems one Si–N pair per formula unit can be replaced by one Al–O pair in accordance with previous findings[29,41,42] while the true solubility limits in the M′(Gd) and M′(Dy) systems seem to be somewhat less (0.75) and even smaller in the M′(Y) system (0.60). These findings also confirm that the limit of aluminum solubility decreases with the ionic radii of the RE element.[43] It was also shown, that the substitution of Si–N by Al–O in the M(R) structure produces a lattice expansion.[36] The fact that the maximum value of lattice expansion was found in the M′(Nd) system (1.66%) and the minimum one in the M′(Y) system (0.70%) further supports the conclusion that the investigated systems exhibit different solid solubility ranges.

A tentative attempt to rationalize the interrelation between the ionic radii of RE element and the solubility limits of different M′(R) phases was made in Ref. 40 and is based on the simple considerations regarding the

structure of melilite-type phases. The projection of the yttrium melilite on (100) may be schematically represented as shown in Fig. 1. With non-bridging anions taking up positions on the apex of the tetrahedra each silicon oxynitride layer of the N-melilite structure possesses an overall negative charge that has to be balanced by the RE cations. These cations separate the silicon oxynitride layers by a finite distance. In systems with small cation sizes such of as yttrium or dysprosium, the negatively charged layers are allowed to come relatively closely together and possibly create a repulsive force which can destabilize the melilite structure. A structurally unstable M′(R) phase may result in a low aluminum accommodation capability. However, the exact mechanism involved in this process is currently unknown.

One of the main issues of interest in regard of the properties of the M′(R) phases is their behavior at high temperatures primarily in relation with densification of respective SiAlON compositions. Al-free melilites tend to become unstable at temperatures exceeding 1800°C. Melting of melilites is thought to be impossible because the edge of the liquid region in the four component R–Si–O–N plane does not reach as far as the melilite composition (i.e., 67 eq.% nitrogen). Instead, the melilite phases are believed to decompose with significant loss of nitrogen, resulting in the formation of J phase. For M′(R), stability at high temperature is determined by two factors. With increasing aluminum content, the limiting composition of M′(R) gradually moves towards the liquid region, and at the same time the liquid region can accommodate a higher nitrogen concentration with increasing temperature, approaching the terminal composition of M′(R). Current preparative evidence suggests that the liquid region eventually reaches the M′(R) composition, and M′(R) melts.[29] This generates large amounts of liquid which, in combination with silicon, nitrogen and other components, promotes the precipitation of α-SiAlON phase and accelerates the final densification. This effect has been widely observed in several SiAlON systems.[41,44]

It is clear that the melting temperature of M′(R) varies in different systems according to the densifying cation, but a low melting temperature for M′(R) is a key factor in the preparation of dense α and αβ-SiAlON ceramics. According to Ref. 29 the M′(Sm) melts at about 1700°C, and on cooling at normal furnace cooling rate M′(Sm) reprecipitates, suggesting that any liquid with M′(R) composition does not form a glass. Although it has not yet been confirmed that dissolution of aluminum in M(R) actually lowers the melting temperature of these phases, but the closeness of the M′(R) composition to the liquid-forming region certainly dominates the behavior of M′(R) phases at high temperatures. As it will be discussed further, the high temperature behavior of M′(R) phases plays an important role in the reversible α′ to β′ transformation in SiAlON ceramics.

Another important factor in designing and processing of various silicon nitride based materials, (α + β)-SiAlONs in particular, are the phase relations of M′(R) with the neighboring phases in different M–Si–Al–O–N systems. The most thorough and systematic research of this subject was accomplished in Refs. 45 and 46. This research covered the majority of RE oxides (R = La, Gd, Dy, Er, Y, Nd, Sm, and Yb) that are used as sintering aids in complex SiAlON systems. Firstly, it was shown that the nominal compositions of N-melilite do not form a single-phase material for neither of the RE

Table 2
Reactions and phase formation in $R_2Si_3O_3N_4$ compositions[46] [a]

Rare-earth element, *R*	Reaction temperature (°C)/time (h)	Appearance	Phase analysis by XRD	M(R) lattice parameter (Å)	
				a	*c*
Lanthanum	1650/2 (Sintering)	White	K, 1:2		
	1550/1.5 (HP)	Gray	K, 1:2		
	1600/1.5 (HP)	Gray	K, 1:2		
	1650/1.5 (HP)	Black	1:2, K		
Neodymium	1550/1.5 (HP)	Blue	M. K (vw)	7.721	5.036
	1700/1.5 (HP)	Blue	M, K (w)		
Samarium	1700/2 (Sintering)	White	M, K (vw)		
	1700/1.5 (HP)	Brown	M, K (vw)	7.695	4.991
Gadolinium	1700/2 (Sintering)	White	M, K (vw)	7.650	4.961
Dysprosium	1700/2 (Sintering)	White	M, J (w)	7.618	4.925
Europium	1700/2 (Sintering)	Pink	M, J, 2:1		
	1700/1.5 (HP)	Pink	M, J (mw)	7.585	4.896
Ytterbium	1700/2 (Sintering)	Black	M, J, 2:1		
	1700/1.5 (HP)	Black	M, J (mw)	7.563	4.876

[a] mw, medium weak, w, weak, vw, very weak, HP, hot pressing.

Table 3
Reactions and phase formation in $R_2Si_2AlO_4N_3$ compositions[46] [a]

Rare-earth element, R	Reaction temperature (°C)/time (h)	Appearance	Phase analysis by XRD	M(R) lattice parameter (Å)	
				a	*c*
Lanthanum	1650/2	Partly melted	1:2, K		
	1600/2	White, not dense	M′, K, 1:2	7.855	5.120
	1550/1.5 (HP)	Gray	K, 1:2, M′		
Neodymium	1650/2	Purple	M′	7.766	5.055
Samarium	1650/2	Brown	M′	7.730	5.014
Gadolinium	1650/2	Gray	M′	7.689	4.993
Dysprosium	1650/2	Yellow	M′, J′ (vw)	7.655	4.955
Yttrium	1650/2	White	M′, J′ (w)	7.629	4.929
Europium	1650/2	Pink	M′, J′ (mw)	7.608	4.920
Ytterbium	1650/2	Black	J′		

[a] mw, medium weak, w, weak, vw, very weak, HP, hot pressing.

elements investigated. Moreover, it was unequivocally shown that M(R) is not formed with lanthanum, which, depending on the synthesis conditions, forms a mixture of K-phase ($La_2O_3{\cdot}Si_2N_2O$) and 1:2 phase ($La_2O_3$2-Si_3N_4) in this or that proportion. The results of the attempts of M(R) synthesis with different RE elements are listed in Table 2.

The tendency for forming different components in high-temperature synthesis can be rationalized using the concept of acid-base reactions.[47] Silicon nitride may be considered as more acidic than Si_2N_2O, which enters the compositions of J ($2R_2O_3Si_2N_2O$) and K ($R_2O_3Si_2N_2O$) phases, formed by different RE elements as "impurity" or additional phases (see Table 2), and light RE oxides as more basic than heavy RE oxides. The various minor phases formed in the presence of melilite then can be viewed as the product of the following reactions:

1:2 phase $La_2O_3{\cdot}2Si_3N_4$ (strong base/strong acid)

K phase $La_2O_3{\cdot}Si_2N_2O$ (strong base/weak acid)

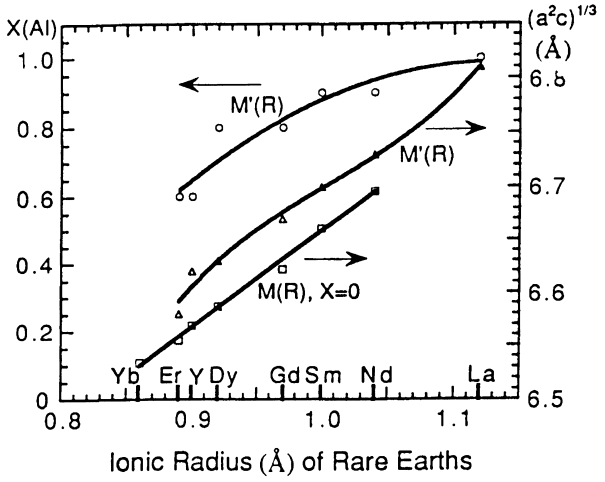

Fig. 2. X(Al) atomic fraction in M′(R) and cell size as a function of ionic radii of rare-earth elements.[46]

J phase $2Y_2O_3{\cdot}Si_2N_2O$ (weak base/weak acid)

For example, as the basicity of R_2O_3 decreases with decreasing ionic radius, it prefers to react with a weak acid to form J phase rather than K phase or 1:2 phase. It is also interesting to note that the molar ratio of base to acid in K(R) and J(R) increases from 1:1 to 2:1; this reflects the need for a larger amount of the weaker base to react with the same acid.

Interesting results and trends were discovered for M′(R) phases when an attempt was made to synthesize the nominal composition $R_2Si_2AlO_4N_3$. M′(R) solid solution was found in all cases except ytterbium (Table 3). Overall, the systematic trend of phase distribution discovered was very similar with the one for M(R), with the minor phases favoring K-phase, in the case of lanthanum, and J-phase, in the case of heavy rare-earth elements. However, some differences were also discovered.

First, in the case of lanthanum, melilite solid solution was formed. This is in contrast with Al-free composition, which did not form La-melilite. The lattice parameters of M′(La) were larger than all of the other M(R) and M′(R) found so far ($a = 7.855$Å and $c = 5.120$Å). The composition of M′ (La) was found to be $La_{1.98}Si_{1.82}Al_{0.96}O_{4.21}N_{3.08}$, i.e., essentially an $x = 1$ compound in the $R_2Si_{3-x}Al_xO_{3+x}N_{4-x}$ series. Similar compositional investigations revealed that the x value decreases monotonically with the atomic number of the RE element. This can be interpreted as a size effect. From the interrelation between the ionic radii of RE elements and both x value and (cubic root of) unit cell volume, $(a^2c)^{1/3}$, from M(R) and M′(R) (Fig. 2) it is evident that the unit cell has expanded in M′(R) relative to M(R). This is accompanied by the substitution of Si–O bond (bond length 1.62Å) and Si–N bond (1.74Å) by Al-O bond (1.75Å). Apparently, in the case of lanthanum, which has a very large radius, only after maximal substitution, $x = 1$, is it possible to incorporate lanthanum into the

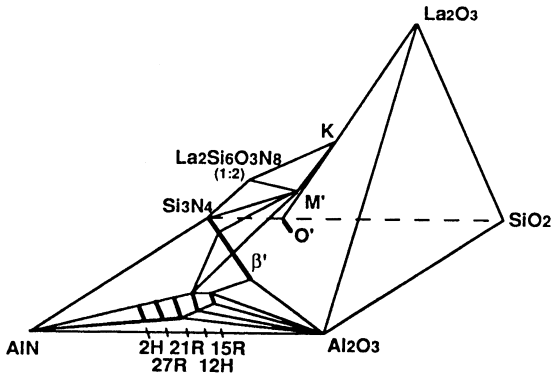

Fig. 3. Phase relations of M′(R) with neighboring phases in R–Si–Al–O–N system.[46]

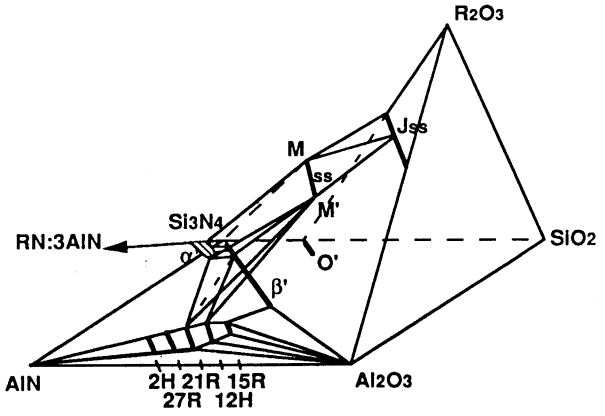

Fig. 4. Phase relations of M′(R) with neighboring phases in R–Si–Al–O–N (R = Gd, Dy, Er, Y) system.[46]

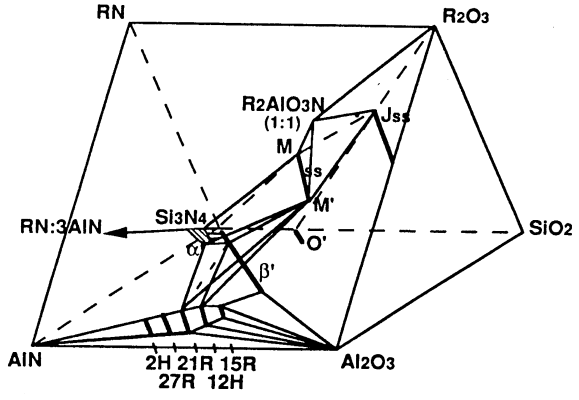

Fig. 5. Phase relations of M′(R) with neighboring phases in R–Si–Al–O–N (R = Nd, Sm) system.[46]

melilite structure. In case of ytterbium, which has a very small radius in contrast, it is apparently stable only in the limit of smallest volume realizable at $x = 0$.

The lattice parameters of melilite and its solid solution obtained for different RE elements at different x values can be correlated to each other, according to Ref. 46, by the following formula:

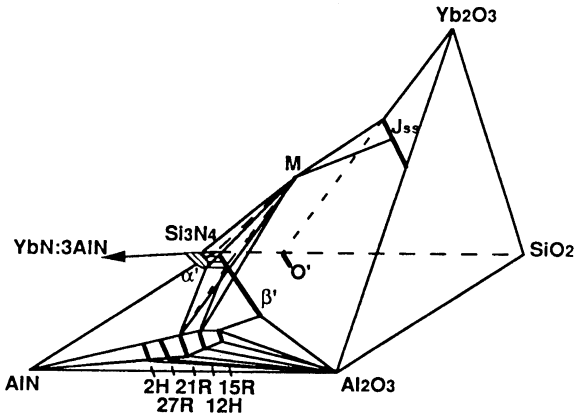

Fig. 6. Phase relations of M′(R) with neighboring phases in Yb–Si–Al–O–N system.[46]

$$a(\text{Å}) = 6.795 + 0.892r + 0.045x$$

$$c(\text{Å}) = 4.121 + 0.874r + 0.033x$$

where r is the ionic radius (in angstroms) of the RE ion using Ahrens scale. These formulas were obtained by a regression analysis of the experimental data on XRD-determined lattice parameters of M(R) and M'(R) formed by different RE elements and can be used for identifying the composition of $R_2Si_{3-x}Al_xO_{3+x}N_{4-x}$ once the identity of the rare-earth element is known.

As to the two other phases, K and J, that were present in the synthesized samples the mechanism of formation and the trends of stability were also formulated in Ref. 46. Formation of K phase was attributed to the reaction of R_2O_3 with the surface-oxidized Si_3N_4, forming Si_2N_2O. In the case of the Al-containing compositions, the oxidized nitride was supposed to be incorporated into M′(R) solid solution thus preventing the formation of the K phase. For J phase, formation of J′(R) solid solutions was confirmed for a number of RE elements. Moreover, it was shown that the stability of both J(R) and J′(R) increases with the decrease of ionic radii of RE elements. The x value for J′(R) was shown to increase with the ionic radius of the RE element, which is similar to the trend found for M′(R).

Recognizing the systematic trends in M′(R), J′(R), α′, and β′ compositions, which vary with different RE elements, a series of tentative diagrams were suggested in Ref. 46 to delineate the phase relationships between melilite and neighboring phases. The RE aluminoxynitride, R_2AlO_3N, denoted as 1:1, was included into consideration, based on the findings of Ref. 48. Four prototypical diagrams, presented in Figs. 3–6, illustrate these relationships:

For lanthanum, there is no α′ solid solution; the $x = 1$ compound of M′(R) forms. In addition, $La_2Si_6O_3N_8$ (1:2 phase) exists as a neighboring phase (see Fig. 3);

For neodymium and samarium, there is an extensive solid solution of both α′ and M′(R), but only J phase, not J′(R) solid solution, is compatible with M′(R). In addition, R_2AlO_3N forms and is compatible with M′(R) and J (see Fig. 4). The compatibility of $RAlO_3$ (R = Nd, Sm) with M′(R) were not resolved. According to Ref. 46, M′(R) is compatible with $RAlO_3$, while according to Ref. 49, $SmAlO_3$ may be just a product that forms on cooling at some specific conditions and, in fact, is not compatible with M′(R). In Ref. 42 only coexistence of M′(R), R_2AlO_3N and J phase at 1550°C was found.

For gadolinium, dysprosium, europium, and yttrium, there was found an extensive solid solution of α′, but the solid solution range of M′(R) was shown to be compatible with M′(R), while the compound R_2AlO_3N failed to form in this case (see Fig. 5).

Ytterbium was shown to enter α′ solid solution and J′(R) solid solution. However, only M(R), not M′(R), was proven to form in this case (see Fig. 6).

3. Subsolidus phase relationships in R_2O_3–Si_3N_4–AlN–Al_2O_3 systems

As already mentioned, the importance of using RE oxides for the densification of silicon nitride ceramics was recognized in recent years. Not only are they very effective along with alumina for densification, either singly or in combination with yttria, but they can also be accommodated in the αSi_3N_4 lattice forming α-SiAlON, thus providing the opportunity for decreasing the transient liquid phase content after sintering and hence reducing the amount of residual grain boundary glass. Therefore, phase relationships in Ln–Si–Al–O–N systems are of particular interest.

Y–Si–Al–O–N system was investigated most thoroughly. Initially, research in this system has been restricted to the region bounded by Si_3N_4, β-SiAlON, Al_2O_3, SiO_2 and Y_2O_3, which does not include the solid solution α-SiAlON. Huang et al. reported the α-SiAlON formation in the system Si_3N_4–AlN–Y_2O_3[50] and Si_3N_4–AlN–RE.[17] The systems Si_3N_4–AlN–Y_2O_3 and Si_3N_4–($AlNAl_2O_3$)–(YN3AlN) have also been studied by the same authors.[51] Later, with the emergence of α-SiAlON, information on the nitrogen-rich part of the Y–Si–Al–N–O system became necessary. Thirty-nine four-phase equilibria, also named compatibility tetrahedra, had

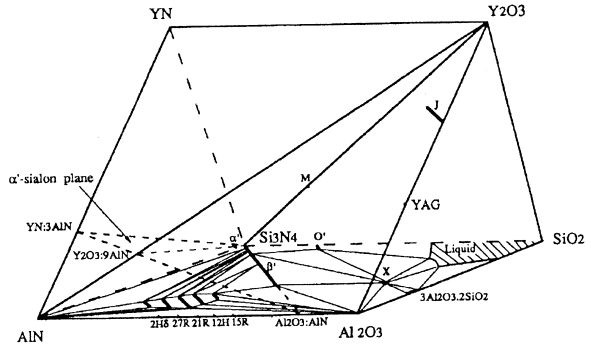

Fig. 7. Representation of Y–Si–Al–O–N system showing phases occurring in the region bound by Si_3N_4, Y_2O_3, Al_2O_3, and AlN, and Si–Al–O–N behavior diagram at 1700°C.[52]

Table 4
Subsolidus compatibility tetrahedra in Si_3N_4–AlN–Al_2O_3–Y_2O_3[52] [a]

Al_2O_3–β_{60}–15R-YAG	Al_2O_3–15R–15R′–YAG
$Al_2O_3$15R′–12H′–YAG	Al_2O_3–12H′–21R′–YAG
Al_2O_3–21R′–AlN–YAG	15R–15R′–12H–12H′–YAG
12H–12H′–21R–21R′–YAG	21R–21R′–27R–27R′–YAG
27R–27R′–2H$^{\delta}$–2H$^{\delta\prime}$–YAG	2H–2H$^{\delta}$–AlN–YAG
21R′–27R′–AlN–YAG	27R′–2H$^{\delta\prime}$–AlN–YAG
21R–27R–YAG–J′(R)	27R–2H$^{\delta}$–YAG–J′(R)
2H$^{\delta}$–AlN–YAG–J′(R)	AlN–YAG–J′(R)–YAM
AlN–YAM–J–Y_2O_3	β_{60}–β_{25}–15R–YAG
β_{25}–15R–12H–YAG	β_{25}–β_{10}–12H–YAG
β_{10}–α′–12H–YAG	α′–12H–21R–β_{10}
α′–21R–β_{10}–β_8	α′–21R–β_8–27R
α′–β_8–27R–β_2	α′–27R–β_5–2H$^{\delta}$
α′–β_5–2H$^{\delta}$–β_2	α′–2H$^{\delta}$–β_2–AlN
α′–β_2–AlN–Si_3N_4	α′–12H–21R–YAG
α′–21R–YAG– M	α′–21R–27R–M
α′–27R–2H$^{\delta}$–M	α′–2H–AlN–M
M–21R–YAG–J′(R)M–21R–27R–J′(R)	M–21R–27R–J′(R)
M–27R–2H$^{\delta}$–J′(R)	M–2H$^{\delta}$–AlN–J′(R)
M–AlN–J′(R)–J	

[a] YAM, $2Y_2O_3{\cdot}Al_2O_3$; J, $2Y_2O_3{\cdot}Si_2N_2O$; J′(R) = $2Y_2O_3{\cdot}Al_2O_3$–$Y_2O_3{\cdot}Si_2N_2O$; M = $Si_3N_4{\cdot}Y_2O_3$; 15R, 12H, 21R, 27R, 2H$^{\delta}$ are Si–rich terminals of AlN polytypoids; 15R′, 12H′, 21R′, 27R′, 2H$^{\delta\prime}$ are Al–rich terminals of AlN polytypoids.

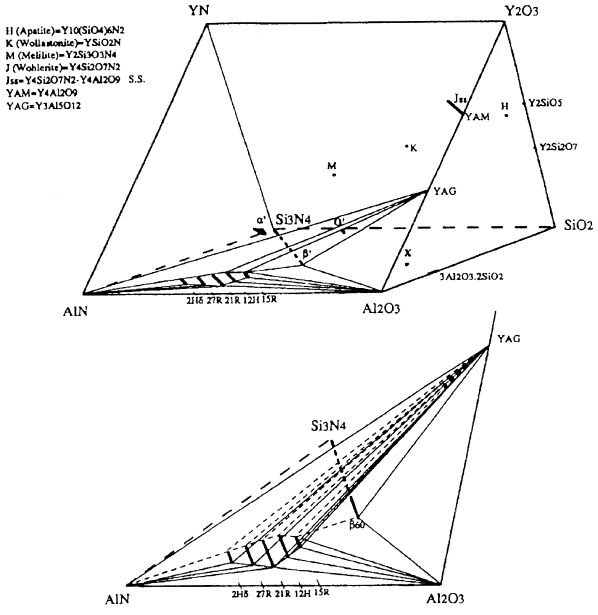

Fig. 8. Representation of compatibility of the YAG with polytypoid phases, AlN, and Al_2O_3, 12 compatibility tetrahedra are formed.[52]

been established in the region Si_3N_4–AlN–Al_2O_3–Y_2O_3 (Table 4).[52] The subsolidus phase relationships in the region Si_3N_4–AlN–YN–Y_2O_3 were also determined. Only one compound, 2YN:Si_3N_4, was confirmed in the binary system Si_3N_4–YN contrary to the early results of Thompson[53] who reported the existence of three compounds: 6YN·Si_3N_4, 2YN·Si_3N_4, and YN·Si_3N_4. This contradiction could be explained by the purity of the YN used as a starting material, and in that case the X-ray diffraction lines of 2YN·Si_3N_4 and YN·Si_3N_4 reported by Thompson may be regarded as a mixture of

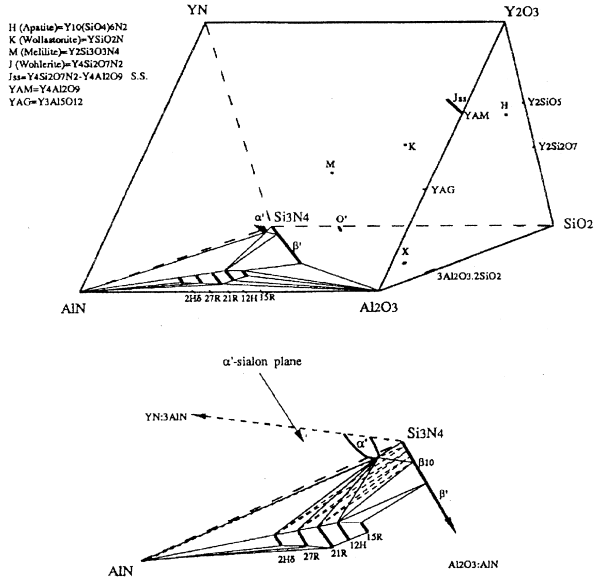

Fig. 9. Representation of compatibility of the α-SiAlON with polytypoid phases (from $2H^{\delta}$ to 12H), AlN, and β′, eight compatibility tetrahedra are formed.[52]

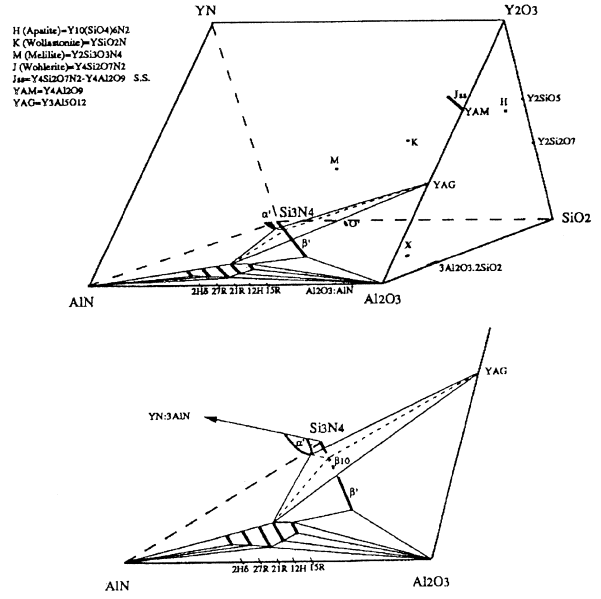

Fig. 10. Compatibility terahedron α′-β_{10}-12H-YAG.[52]

melilite ($Y_2Si_3O_3N_4$), J phase ($2Y_2O_3{\cdot}Si_2N_2O$), and other oxygen-containing phases. The solubility limits of the α-SiAlON on the Si_3N_4–YN3AlN join were determined to range from $m = 1.3$ to 2.4 in the formula $Y_{m/3}Si_{12-m}Al_mN_{16}$. No quinary compounds were found. Seven compatibility tetrahedra were established in the region Si_3N_4–AlN–YN–Y_2O_3 (Table 4).

Sixty-eight compatibility tetrahedra were established in the system Y–Si–Al–N–O: 39 in the region bounded by Si_3N_4, SiO_2, AlN, Al_2O_3, and Y_2O_3, seven in the region bounded by Si_3N_4, AlN, YN, and Y_2O_3, and 22 in the region Si_3N_4, β_{60}, Al_2O_3, SiO_2, and Y_2O_3. (here and further β_n with $n = 0$–60 is the denomination of β-SiAlON solid solution proposed in Ref. 7; n value indicates the degree of Si–N for Al–O substitution). All this data are graphically presented in Figs. 7–11.

Subsolidus phase relationship in R_2O_3–Si_3N_4–AlN-Al_2O_3 systems until now were thoroughly investigated for most of RE elements, although not in such a detailed and profound way as the Y-doped one. The determination of the whole system, represents a very large amount of work and most initial studies have restricted to the sub-systems R–Si–O–N, R–Al–O–N (R = Ce, Pr, Nd and Sm) and some planes involving α and β-SiAlON.[17,41] It is known that elements in the lanthanide series are similar to yttrium in compound formation and phase relationships. Previous research on R–Si–O–N subsystems,[54] indicates that the phase relationships are nearly the same as in the Y–Si–O–N system, but in R–Al–O–N systems[55] the phase relationships were shown to vary with atomic number of the rare earth element. The phase relationships in the systems with high Z-value of the rare earth element are similar to those in Y–Al–O–N.[56] In the systems R–Al–O–N (where R = Ce to Sm) to nitrogen containing compounds exist — R_2AlO_3N and $R_{12}Al_{12}O_{18}N_2$ (magneto-plumbite, MP compound) — and no garnet phase occurs; instead the 1:1 aluminate phase becomes stable.[55] The R_2AlO_3N and MP compounds do not occur in those systems containing rare earth oxides with cations smaller than that of Gd.[17,55] Therefore, in the five-component systems with the low Z-value rare earth elements, the phase

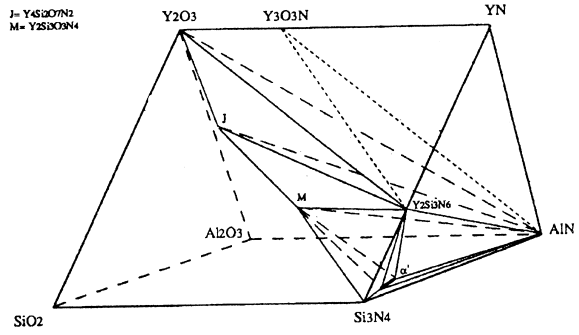

Fig. 11. Subsolidus phase relationships in the region bound by Si_3N_4, AlN, YN, and Y_2O_3.[52]

Table 5
Subsolidus compatibility tetrahedra in the systems Si_3N_4–AlN–Al_2O_3–R_2O_3 (R = Nd and Sm)[59] [a]

Al_2O_3–β_{60}–15R–MP	Al_2O_3–15R–15R′–MP
$Al_2O_3$15R′–12H′–MP	Al_2O_3–12H′–21R′–MP
Al_2O_3–21R′–AlN–MP	15R–15R′–12H–12H′–MP
12H–12H′–21R–21R′–MP	21R–21R′–27R–27R′–MP
27R–27R′–2H$^{\delta}$–2H$^{\delta'}$–MP	2H$^{\delta}$–2H$^{\delta'}$–AlN–MP
21R′–27R′–AlN–MP	27R′–2H$^{\delta'}$–AlN–MP
AlN–2H$^{\delta}$–MP–$LnAlO_3$	2H$^{\delta}$–27R–MP–$LnAlO_3$
27R–21R–MP–$LnAlO_3$	21R–12H–MP–$LnAlO_3$
12H–15R–MP–$LnAlO_3$	β_{60}–15R–MP–$LnAlO_3$
β_{60}–Al_2O_3–MP–$LnAlO_3$	β_{60}–β_{25}–15R–$LnAlO_3$
β_{25}–15R–12H–$LnAlO_3$	β_{25}–β_{10}–12H–$LnAlO_3$
β_{10}–12H–$LnAlO_3$–M′(R)	β_{10}–12H–21R–M′
α'–β_0–β_{10}–M′	α'–β_{10}–21R–M′
α'–β_{10}–β_8–21R	α'–β_8–21R–27R
α'–β_8–β_5–27R	α'–β_5–27R–2H$^{\delta}$
α'–β_5–β_2–2H$^{\delta}$	α'–β_2–2H$^{\delta}$–AlN
α'–β_2–β_0 AlN	α'–AlN–2H$^{\delta}$–M′
α'–2H$^{\delta}$–27R–M′	α'–27R–21R–M′
M′–12H–21R–$LnAlO_3$	M′–21R–27R–$LnAlO_3$
M′–27R–2H$^{\delta}$–$LnAlO_3$	M′–2H$^{\delta}$–AlN–$LnAlO_3$
M′–AlN–$LnAlO_3$–J(R)	M′–AlN–J(R)–M
AlN–$LnAlO_3$–J(R)–Ln_2AlO_3N	$LnAlO_3$–J(R)–Ln_2AlO_3N–Ln_2O_3

[a] MP; $LnAl_{12}O_{18}N$; M′, $Ln_2Si_{3-x}Al_xO_{3+x}N_{4-x}$; J(R), $Ln_4Si_2O_7N_2$; 15R, 12H, 21R, 27R, 2H$^{\delta}$ are Si–rich terminals of AlN polytypoids; 15R′, 12H′, 21R′, 27R′, 2H$^{\delta'}$ are Al–rich terminals of AlN polytypoids.

relationships become slightly different from those in Y–Si–Al–O–N. In the oxygen-rich region where two five-component phases[57,58] — U phase ($R_3Si_{3-x}Al_{3+x}O_{12+x}N_{2-x}$) and W phase ($R_4Si_9Al_5O_{10}N$) — exist, the former is stable for rare earth cations between La and dysprosium the latter stable only in lanthanum, cerium and neodymium systems. None of the phases above occurs in the yttrium system. The stability of N-melilite ($R_2Si_{3-x}Al_xO_{3+x}N_{4-x}$) in different RE systems was discussed in the previous section of this paper.

Most closely and most recently the subsolidus phase relationships were studied in neodymium and samarium,[59] and dysprosium[60] containing R_2O_3–Si_3N_4–AlN–Al_2O_3 systems. The attention paid to the former two elements is caused by the efforts to substitute yttrium by some cheaper RE elements in Si_3N_4based ceramics without hindering the properties. Dysprosium containing system was chosen because dysprosium is one of the central elements in the RE series: in this region, phase relationships in R–Si–Al–O–N systems are changing from those observed for the low-Z elements (La, Nd, Sm) to those observed for high-Z elements (Er, Yb... and Y). It was therefore interesting to find out whether these changes occur simultaneously or whether there is overlap in this region between the different phase relationships observed for the high-Z and low-Z rare earths.

According to Ref. 59, samarium has the same behavior as neodymium in regard of phase formation, but it was noted that melting temperatures were lower in the

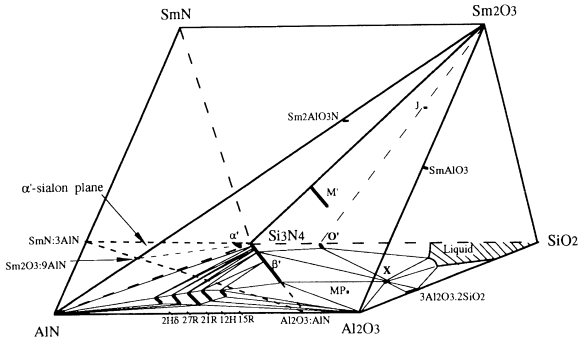

Fig. 12. Representation of Sm(Nd)–Si–Al–O–N system showing phases occurring in the region bound by Si_3N_4, $Sm(Nd)_2O_3$, Al_2O_3, and AlN, and Si–Al–O–N behavior diagram at 1700°C.[59]

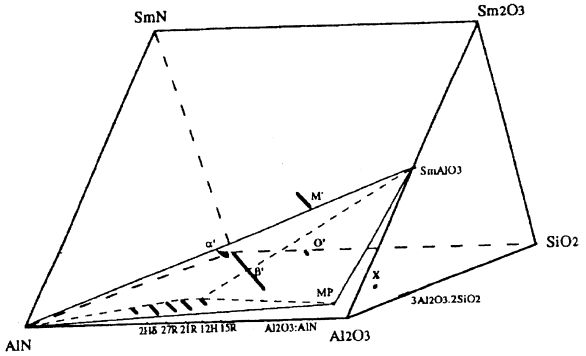

Fig. 13. $Sm(Nd)_2O_3$ is compatible with all polytypoid phases (Si-rich terminal), AlN, and $Sm(Nd)Al_{12}O_{18}N$ (MP compounds) forming five

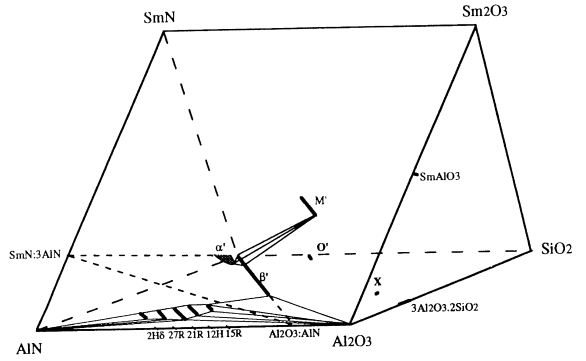

Fig. 14. M′ (melilite solid solution) is compatible with β-SiAlON β_0-β_{10} and α–SIAlON forming α'-β'-M′ compatibility tetrahedron.[59]

samarium-containing system and consequently, at a given temperature, the size of the liquid-forming region is larger. For both samarium and neodymium containing systems, 44 compatibility tetrahedra were established (Table 5). Some specific features of the systems investigated as compared to the Y–Si–Al–O–N system were discovered. Unlike the yttrium containing system where J phase, or woehlerite ($Y_4Si_2O_7N_2$), forms a continuous solid solution with YAM ($Y_4Al_2O_9$) in neither the Sm- nor the Nd- containing system was the formation of such solid solutions observed, although the J phase itself

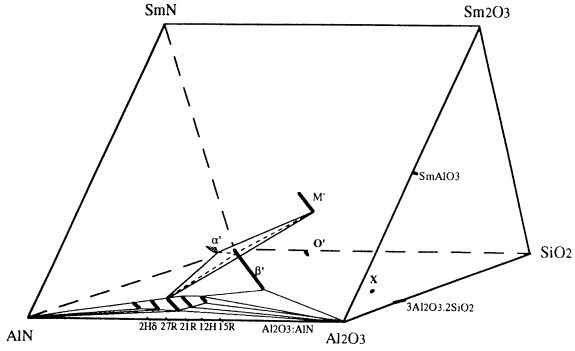

Fig. 15. Compatibility tetrahedron α′-β21-RM′.[59]

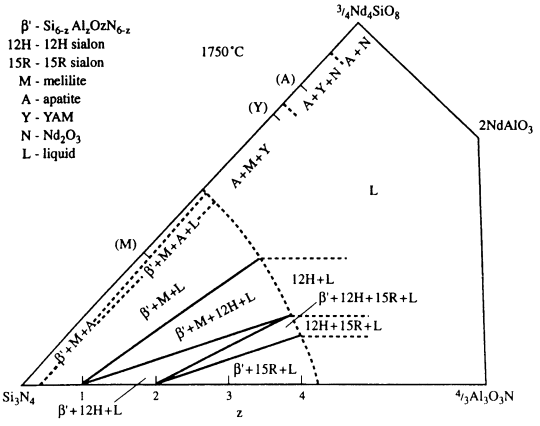

Fig. 16. Phase relationships of β′-$NdAlO_3$ plane at 1750°C. [59]

was readily formed. The N-melilite solid solution M′(R) was found to be compatible with β-SiAlON phase only in the range β_0–β_{10}. Moreover, according to the XRD data Nd- and Sm- melilite (Ln_2O_3–Si_3N_4) seems to have priority over βSi_3N_4 in accommodating aluminum and oxygen [thereby forming M′(R) phase] and therefore the tie lines between melilite and β-SiAlON do not run parallel. The tie line between βSi_3N_4 and $SmAlO_3$ was proven not to exist on account of the results of heat treatment of a number of relevant compositions at 1350 and 1550°C that resulted in formation of M′(R) and apatite [$Sm_{10}(SiO_4)_6N_2$] only. Graphically these results are presented in Figs. 12–16.

In the Dy–Si–Al–O–N system the region defined by the four end-members Si_3N_4, AlN, Al_2O_3 and Dy_2O_3, that includes the phases α-SiAlON, β-SiAlON and AlN polytypoids, and covers the range of compositions used for the design and processing of commercial multi-phase SiAlON ceramics was investigated.[60] The binary tie-lines and 42 compatibility tetrahedra were established based on experimental results and on the more extensive knowledge of phase relationships in the Y–Si–Al–O–N and Sm(Nd)–Si–Al–O–N systems (Table 6).

The DyAG ($Dy_3Al_5O_{12}$) phase is stable and compatible with all the AlN polytypoid phases, β-SiAlON

Table 6
Subsolidus compatibility tetrahedra in the system Si_3N_4–AlN–Al_2O_3–Dy_2O_3[60] [a]

Al_2O_3–β_{60}–15R–DyAG	Al_2O_3–15R–15R′–DyAG
$Al_2O_3$15R′–12H′–DyAG	Al_2O_3–12H′–21R′–DyAG
Al_2O_3–21R′–AlN–DyAG	15R–15R′–12H–12H′–DyAG
12H–12H′–21R–21R′–DyAG	21R–21R′–27R–27R′–DyAG
27R–27R′–2Hδ–2Hδ′–DyAG	2H–2Hδ–AlN–DyAG
21R′–27R′–AlN–DyAG	27R′–2Hδ′–AlN–DyAG
β_{60}–β_{25}–15R–DyAG	β_{25}–15R–12H–DyAG
β_{25}–β_{10}–12H–DyAG	β_{10}–12H–21R–α′
21R–β_{10}–β_8–α′	β_8–21R–27R–α′
27R–β_8–β_5–α′	β_5–27R–2Hδ–α′
2Hδ–β_5–β_2–α′	β_2–2Hδ–AlN–α′
AlN–β_2–β_0–α′	β_0–β_{10}–α′–M′
β_{10}–12H–α′–DyAG	12H–21R–α′–DyAG
21R–27R–α′–M′	27R–2Hδ–α′–M′
2Hδ′–AlN–α′–M′	AlN–2Hδ–M′–DyAP
2Hδ′–27R–M′–DyAP	27R–21R–M′–DyAP
AlN– 2Hδ′–DyAP–DyAM	2Hδ–27R–DyAP–DyAG
27R–21R–DyAP–DyAG	21R–M′–DyAG–DyAP
21R–α′–M′–DyAG	α′–β_{10}–DyAG–M′
J′(middle)–DyAM–DyAP–AlN	Dy_2O_3–J′(whole)–AlN
J–J′(middle)–M–M′–AlN	J′(middle)–M′–DyAP– AlN

[a] DyAM = $Dy_4Al_2O_9$; DyAP = $DyAlO_3$; DyAG = $Dy_3Al_5O_{12}$; 15R, 12H, 21R, 27R, 2Hδ are Si–rich terminals of AlN polytypoids; 15R′, 12H′, 21R′, 27R′, 2Hδ′ are Al–rich terminals of AlN polytypoids.

(from β_{10} to β_{60}) and α-SiAlON (oxygen-rich) forming 12 Al-polytypoids-containing compatibility tetrahedra (Fig. 17) and one α′–β′-containing compatibility tetrahedron, α′–β_{10}–DyAG12H (Fig. 18) unlike the Sm(Nd)-containing systems where the *YAG* does not occur. The melilite solid solution M′ is compatible with both β and α-SiAlON phases, and with DyAG forming two compatibility tetrahedra: α′β_0-β_{10}-M′ and α′β_{10}-M′-DyAG (Fig. 19). Moreover, in the Dy-containing system the J-phase ($Dy_4Si_2O_7N_2$) forms a continuous solid solution with $Dy_4Al_2O_9$ unlike the Sm(Nd)-containing ones and similar with Y and Yb.[32,56,61]. It was also shown that the compound $DyAlO_3$ is compatible only with M′ (melilite solid solution) and Dy-rich terminals of AlN polytypoids (from AlN to 21R), and therefor the tie line between $LnAlO_3$ and β′ that occurs in the Nd(Sm)–Si–Al–O–N systems does not exist in the Dy–Si–Al–O–N system. All the results are summarized in Fig. 20.

Subsolidus phase relationships for other RE elements, although not studied in such detail as the ones presented above, could be easily derived by analogy if the RE element ionic radius is taken into account appropriately.

4. Thermal stability of RE-α-SiAlONs and the reversibility of α′ to β′ transformation

The RE densification additives used for sintering of SiAlON ceramics are generally insoluble in the β-SiAlON structure and even though most of them are α-

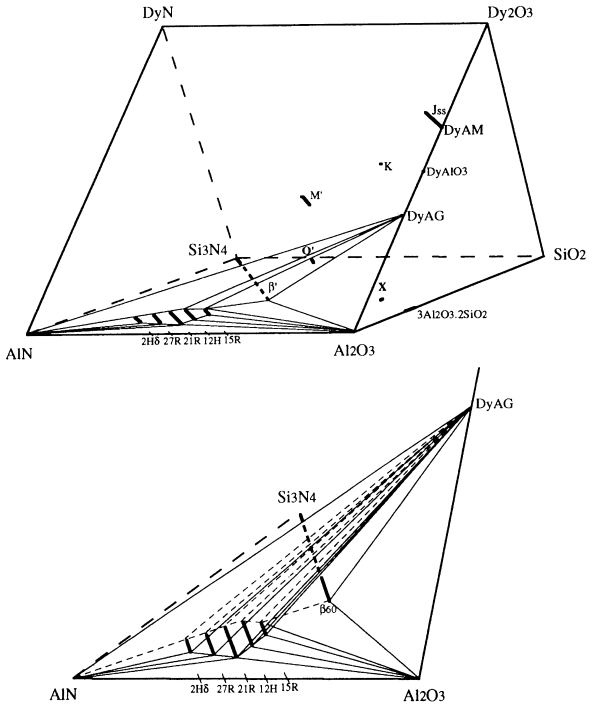

Fig. 17. Graphic representation of compatibility of the DyAG with polytypoid phases, AlN, and Al_2O_3, 12 compatibility tetrahedra are formed.[60]

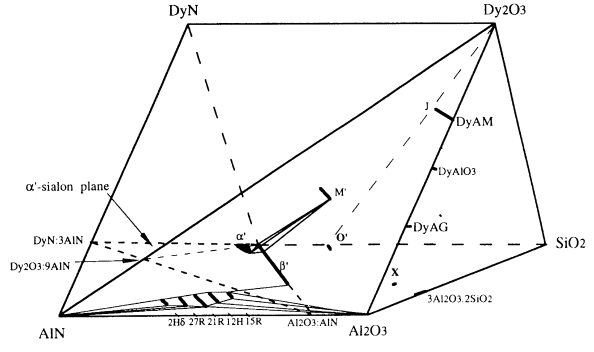

Fig. 18. DyAG is compatible with β-SiAlON β_{10}–β_{60} and α–SiAlON (oxygen-rich) forming α′-β_{10}-12H-DyAG compatibility tetrahedron.[60]

SiAlON formers, some amount of additives remains as a residual M–Si–Al–O–N intergranular glassy phase, which degrades the mechanical and chemical properties of the material above the glass-softening temperature, which normally is about 900–1100°C.

Post-sintering heat treatment is one of the accepted methods to eliminate or minimize the glassy grain boundary phase in nitrogen ceramics by converting it into refractory crystalline phase(s), thus improving the materials performance at elevated temperatures. This is usually achieved via a conventional glass-ceramic process during which the glass devitrifies at a temperature above its T_g point but without being melted.[58,62] There has been much work in understanding of the grain boundary crystallization, but very little attention has

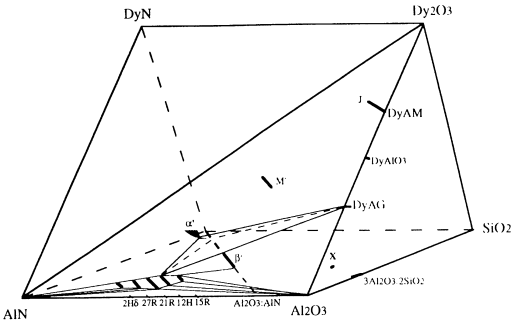

Fig. 19. M′ (melilite solid solution) is compatible with β-SiAlON β_0-β_{10} and α–SiAlON forming α′-β′-M′ compatibility tetrahedron.[60]

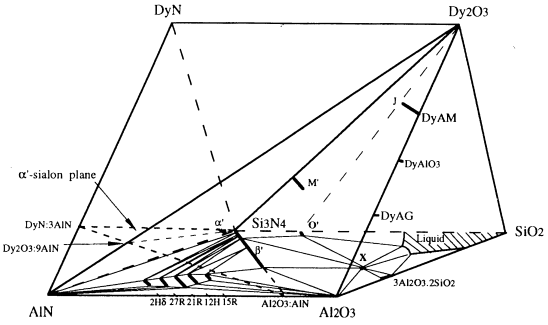

Fig. 20. Representation of Dy–Si–Al–O–N system showing phases occurring in the region bound by Si_3N_4, Dy_2O_3, Al_2O_3, and AlN, and Si–Al–O–N behavior diagram at 1700°C (α-SiAlON plane = the plane with α-SiAlON composition $Dy_xSi_{12-(m+n)}Al_{m+n}O_nN_{16-n}$).[60]

been paid to the effects of the post-sintering heat treatment on the stability of SiAlON phases, while the characterization of the finished product has always focused on the account of the residual glass and the type, amount and microstructure of the resulting crystalline oxynitride phase. However, in the course of the study of densification and post sintering heat treatment of (α + β)-SiAlON compositions containing selected RE additives (Yb_2O_3, Dy_2O_3, Sm_2O_3 either singly or in combination with Y_2O_3). Mandal et al.[25] reported that the transformation from α′ to β′ readily occurred in some RE-(α′ + β′) composite materials when heat treated between 1000 and 1600°C and that extent of the transformation was more pronounced with increasing temperatures.

Although the structure of both α′ and β′ phases are basically built up of corner sharing (Si, Al)(O, $N)_4$ tetrahedra, there is a distinct difference in the atomic arrangement between the two phases.[63,64] The transformation between α′ and β′ phases has a reconstructive nature, which involves the breaking of chemical bounds and substantial atomic diffusion, and hence requires significant amounts of thermal energy. As a result of the strong covalent nature of the bounding associated with both the α′ and β′ structures, the atomic diffusivity of the species making up the lattices is inherently low. It is,

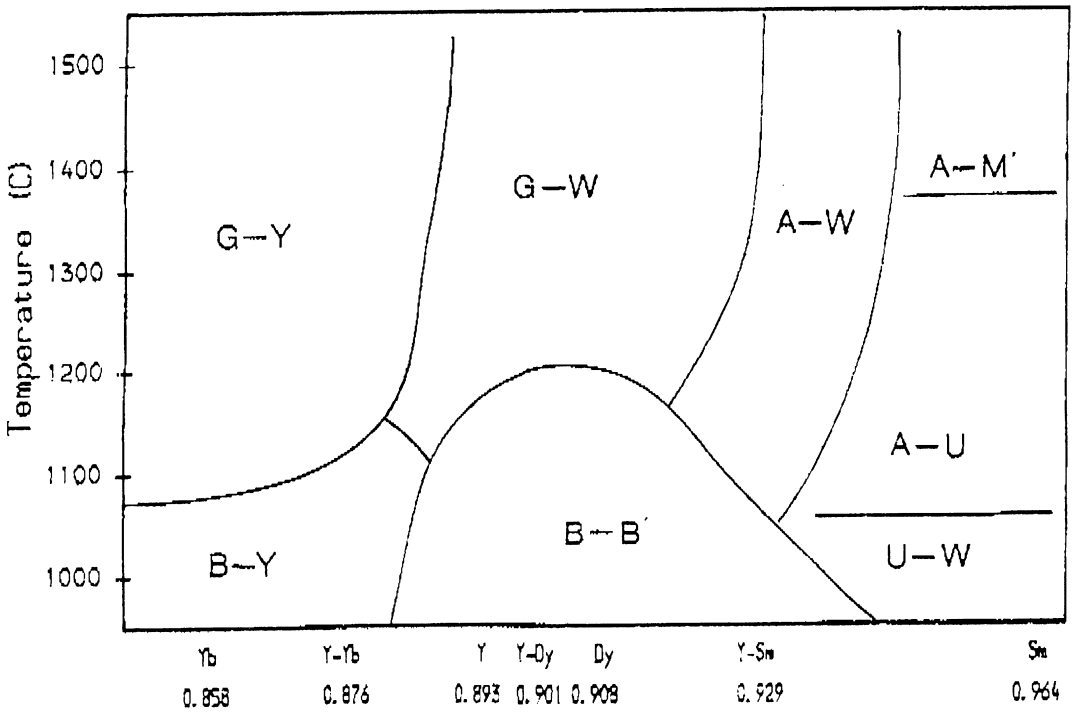

(a)

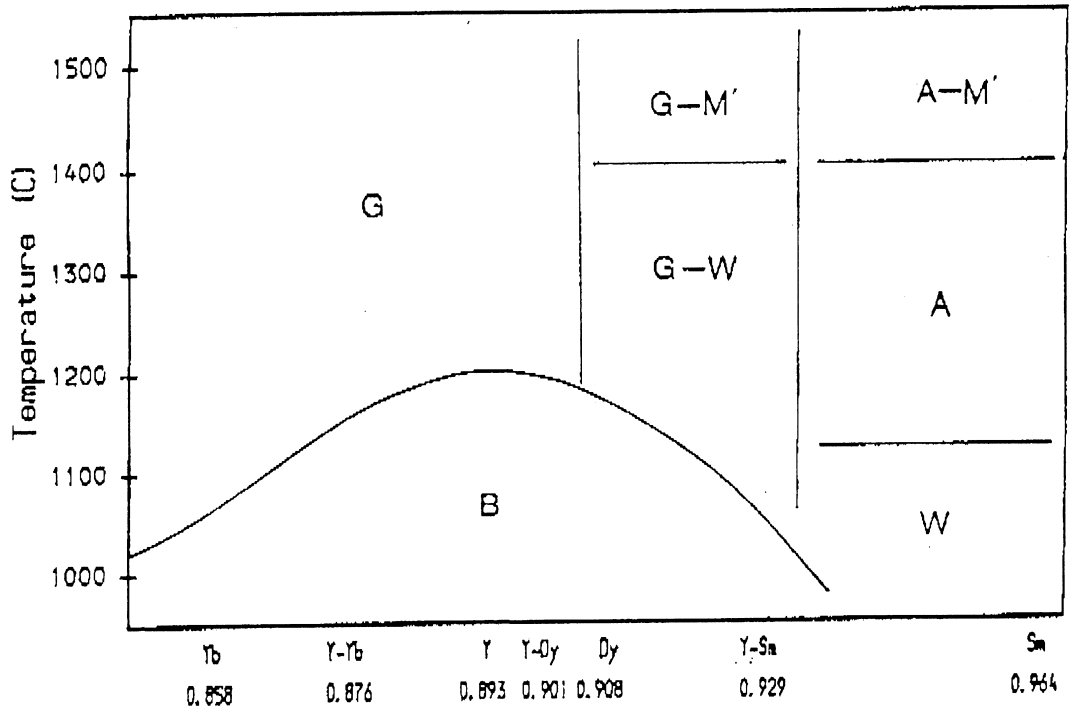

(b)

Fig. 21. Heat treatment of 1775°C pressureless sintered (a) β-SiAlON and (b) α + β-SiAlON materials. B,B-phase {(Y, R)$_2$SiAlO$_5$N}; W, wollastonite {(Y, R)SiO$_2$N}; U, U-phase {R$_3$Si$_3$Al$_3$O$_{12}$N$_2$}; Y, J(R)-phase {(Y < R)Si$_2$O$_7$N$_2$}; G, garnet {(Y, R)$_3$Al$_5$O$_{12}$}; A, aluminate {RAlO$_3$}; and M', melilite {R$_2$Si$_3$O$_3$N$_4$}; with some substitution of Si and N by Al and O.[25]

therefore, generally assumed that the α′ to β′ phase transformation requires a liquid phase to assist the necessary atomic diffusion by analogy with the transformation from α-Si_3N_4 to β-Si_3N_4, which did not occur without the presence of a liquid phase in which α-Si_3N_4 grains could dissolve above ~1400°C.[65] However, the actual role of liquid phase in α′ to β′ transformation has not been fully understood.

According to the observations of Ref. 25, fast cooling (cooling rate of ~ 450°C/min in the interval 1775–900°C) of RE-SiAlON samples performed in order to preserve the intergranular phase in a fully amorphous condition led to a marked increase of the α′-phase content. Thus the original samples designated β-SiAlON being reheated to the sintering temperature and rapidly cooled contained some α-SiAlON, and the original samples designated (α+β)-SiAlON were almost pure α-SiAlON. The effect was more marked in the case of samples densified with higher atomic number rare earths. Subsequent annealing of these samples at various temperatures in the range 1000–1800°C yielded the α′ to β′ transformation accompanied by crystallization of various secondary phases. Both the extent of the α′ to β′ transformation and the resulting secondary phase assembly were obviously dependent on the RE used, specifically the ionic radius of the RE element. The degree of the α′ to β′ transformation was again more pronounced for the higher atomic number RE sintering additives.

The dependence of the phase assemblages after heat treatment on the RE used is presented in Fig. 21. Therefore, it was concluded that the α-SiAlON phase is only stable at high temperatures (typically in excess of 1550°C) and that it transforms to β-SiAlON plus other RE-rich grain boundary phases at lower temperatures.

Further experiments showed that the amount of grain boundary liquid phase in the sample had marked effects on the transformation, and the introduction of an additional amount of glass into a previously stable α′ composition could significantly destabilize the α′ phase and promote the α′ to β′ transformation.[28] After comparing the results in different RE-SiAlON systems, it was further suggested by the same authors that the residual grain boundary liquid phase was one of the most important factors influencing the transformation. The rate of the transformation was stated to be dependent on the amount and viscosity of the intergranular liquid phase present during the heat treatment.

Shen et al.[66] on the other hand, proposed two possible transformation routes, one involving a liquid phase, i.e. α′ + liquid β′ + M′ and other being a direct decomposition of the α′ phase to form β′ and the aluminum-containing melilite [$Sm_2Si_{3-x}Al_xO_{3+x}N_{4-x}$, M′(R)] phases in the Sm (α+β)- SiAlON system, without the involvement of a liquid phase. However, a more in-depth investigation of the thermal decomposition of samarium and ytterbium stabilized α-SiAlON phases revealed that some self-generated liquid phase is involved in the process of α′ to β′ transformation.[67] Unique microstructural features resulting from the α- to β-SiAlON transformation have been observed in Sm- and Yb-(α+β)-SiAlON samples. The newly formed β′-grains, namely the ones formed as a result of α′ to β′ transformation, contain a high density of dislocations and a large amount of ultrafine (~40 nm) spherical inclusions which are often associated with dislocations. The conclusion that such microstructure is a unique feature associated with the α′ to β′ transformation was based on careful structural analyses by several methods. It was also shown that the transformed grains grow as a result of the epitaxial heterogeneous nucleation on the pre-existing β′ phase.

According to Ref. 68, the α′ to β′ transformation occurs in two stages. The first stage involves relatively high amounts of intergranular glassy phase, which provides the liquid phase necessary for transformation since the post-sintering heat treatment is conducted at the temperatures exceeding the melting point of the glass. At this stage the transformation occurs according to the mechanism described above.[66] After the initial period of heat treatment, the volume percentage of the residual grain boundary glass is reduced dramatically; hence its role in the transformation would be severely restricted. Moreover, the M′(R) phase formed during the first stage is very stable at the annealing temperatures that have been applied (1450°C). Once it has formed it would not re-melt to become a liquid grain boundary phase and to be involved in α′ to β′ transformation at this temperature.[48,66] The rate of the α′ to β′ transformation at the second stage, i.e. after devitrification of the intergranular glass was accomplished, was observed to be somewhat lower than at the first stage but the process continued at a nearly constant rate, suggesting additional mechanism(s) to be operative until the system is closed to equilibrium. The activation energy of a reconstructive phase transformation will be significantly reduced if the atomic diffusion is assisted by a liquid phase and/or it there exist nuclei to reduce the interfacial energy. The occurrence of the self-generated liquid in transformed β′ grains leads to a logical assumption that this liquid phase plays a major role in promoting atomic diffusion and facilitating α′ to β′ transformation after crystallization of the grain boundary liquid. Because it involves a liquid phase emerging from the transforming α′ phase itself, the transformation from α′ to β′ can be proceed without involving much grain boundary liquid and a steady rate of the transformation may be expected.

The appearance of the RE-rich spheroids in the β′ phase results in thermodynamic instability, hence these nano-sized inclusions would eventually diffuse out of the transformed β′ grains through the easy path of dislocations. It is therefore, suggested in[68] that the amount and viscosity of the self-generated liquid within the

transforming α′ grains is a determining factor in controlling the rate of the α′ to β′ transformation when most at the grain boundary glass has been crystallized.

Without much involvement of grain boundary glass, the α′ to β′ transformation at the second stage may be regarded as a decomposition process of α-SiAlON phases. This suggests that, below a certain temperature, some of the α′ compositions have a higher free energy than β′ phases, and the transformation from α′ to β′ would occur if it could be thermally activated. Because of the compositional difference between α′ and β′ phases, the transformation of α′ into β′ must produce additional phases(s). If in Ref. 66 it was suggested that α′ decomposes with the formation of α′ and M′(R), the more recent investigations in the Sm–Si–Al–O–N system[68] where the EDS X-ray mapping technique was applied for quantification of AlN polytypoid phases showed that another, more complicated, reaction path seems to be more plausible for description of Sm- α′-SiAlON phases decomposition, namely $\alpha' \xrightarrow{\text{internal liquid}} \beta' + M' + 21R_{AlN}$.

Further attempts to reach even more complete understanding of the mechanism of this interesting transformation together with the evaluation of different rare-earth-doped duplex (α + β)-SiAlONs for long term high temperature stability are presented in Refs. 69 and 70. Both aspects are of special interest since many applications for (α-β)-SiAlON ceramics are in the temperature range where the α′ to β′ transformation will continue with consequent continuous change in properties. The research accomplished in Ref. 69 was mostly aimed at elucidation of the effect of starting composition, type of rare earth sintering additive and amount of liquid phase on the α′ to β′ transformation during post sintering heat treatment. Therefore, five different (α + β)-SiAlON and α-SiAlON compositions have been prepared using neodymium, samarium, dysprosium and ytterbium. The reasons for preparation of these compositions were as follows:

- first group was formulated as the original starting composition used in Ref. 25 and has been shown to readily undergo α′ to β′ transformation;
- the second group was formulated to produce a phase composition of approximately, 30% α-SiAlON and 70% β-SiAlON;
- the third was also aimed for the two-phase region but was more α-SiAlON rich (≈ 50% α-SiAlON and 50% β-SiAlON); this composition was useful for comparison with the first two compositions to understand the effect of liquid phase, since the amount of liquid is less and the viscosity is higher than in the other two;
- the fourth group was formulated for an α-SiAlON with $m = 1$ and $n = 1.7$ (oxygen-rich corner of the α-SiAlON phase region) and was designed to determine whether all different cation size RE sintering additives give pure α-SiAlON, since the borders of α-sialon phase field have only been established precisely in the yttrium system;
- the fifth group was designed as an α-SiAlON composition with $m = 1.5$ and $n = 1.5$, representing the maximum nitrogen content α-SiAlON composition which can be prepared without RE element nitride additions.

A combination of extensive X-ray and microstructural observations on sintered and heat treated samples showed that the α-SiAlON composition in mixed (α + β)-SiAlON materials is always located at the edge of the α-SiAlON phase region and is less stable with respect to α′ to β′ transformation than in single phase α-SiAlON phase region. For (α + β)-SiAlON composites the transformation was shown to proceed more readily with the increase of the amount and the decrease of the viscosity of liquid phase formed during heat treatment. For the α-SiAlON starting compositions prepared both within or the edge of the α-SiAlON phase

Table 7
Mechanisms influencing α′ to β′ transformation[69]

Sample	O:N ratio (%)	Sintering additive	α′ to β′ transformation	Driving force		
				R cation size	Amount and viscosity of liquid phase	β-SiAlON nucleation sites
R1	13.7	Nd_2O_3 or Sm_2O_3	+	+ + +	+ +	+
		Dy_2O_3 or Yb_2O_3	+	No	+ + +	+
R2	10.6	Nd_2O_3 or Sm_2O_3	+	+ + +	+ +	+
		Dy_2O_3 or Yb_2O_3	+	No	+ + +	+
R3	9.12	Nd_2O_3 or Sm_2O_3	+	+ + +	+ +	+
		Dy_2O_3 or Yb_2O_3	+	No	+ + +	+
R4	11.88	Nd_2O_3 or Sm_2O_3	+	+ + +	+ +	+
		Dy_2O_3 or Yb_2O_3	+	No	+ +	+ + +
R5	10.34	Nd_2O_3 or Sm_2O_3	+	+ + +	+ +	No
		Dy_2O_3 or Yb_2O_3	No	No	No	+ + +

region, the regularities of the ease of phase transformation are of a more complex nature. A combination of three factors influences the ease of transformation: the cation size of the sintering additive, the presence of β-SiAlON grains and also the amount and viscosity of liquid phase present during heat treatment. The role of the liquid phase in the phase transformation for all compositions was elucidated in the same way: an extra amount (10 and 20%) of glass powders of overall composition R: Si: Al = 1:1:1 was added to the samples. Such additions led to unequivocal intensification of the α′ to β′ transformation in all samples with the exception of the ones from the fifth group (see above), that were doped with small ionic size of sintering additives (Dy_2O_3 and Yb_2O_3). For these materials the presence of β-SiAlON grains was necessary for triggering the transformation. Moreover, the increase of the number of such grains (10% β-SiAlON with $z = 0.8$ was added to one of the mixtures) enhanced the transformation substantially, while such grains might possibly act as a nucleation site for α′ to β′ transformation. Only then the amount and viscosity of liquid became important factors for the overall reaction α-SiAlON + β-SiAlON + ($21R_{AlN}$) + liquid → β-SiAlON + ($21R_{AlN}$) + grain-boundary phase(s). β-SiAlON nucleation sites provided more favorable kinetic conditions for transformation in case of large ionic size sintering additives, but the process itself proceeded without any additional ones. The overall results are summarized in Table 7, where increasing number of "+" marks indicate the more dominant mechanism influencing α′ to β′ transformation.

Somewhat similar research was carried out for duplex (α + β)-SiAlON composites stabilized with neodymium, ytterbium, and yttrium. The former two RE elements were chosen because they represent the size end members of rare earth cations known to stabilize α′, while yttrium served as a reference. The long-term high-temperature stability of the different duplex (α + β)-SiAlON ceramics was of special interest. Phase and microstructural development and the volume fraction and chemistry of residual intergranular phases were characterized and related to mechanical properties. It was shown that on sintering the duplex (α + β)-SiAlON starting powder compositions result in equilibrium phase compositions consisting of α′, β′ and a residual glassy phase. The analytical XRD investigations showed that α′ and β′ substitution levels and the equilibrium composition and volume fraction of the glass are dependent upon the starting composition as well as the α′ stabilizing cation. However, the β′/(α′ + β′) weight ratio was shown to depend mostly on the RE element used. The long-term heat treatment experiments at 1450°C clearly indicate that yttrium and ytterbium give a stable α-SiAlON phase, while neodymium gives a less stable one that during prolonged heat treatment at 1450°C decomposes into crystalline phases: melilite, β-SiAlON, and 21R polytypoid. These observations are fully consistent with the results of Ref. 69. Overall, the above described experimental results on the stability of α′ and α′ to β′ transformations strongly indicate that for duplex (α + β)-SiAlON composites designed for high-temperature applications RE elements with smaller ionic radii present an optimal choice.

It must be also noted that in spite of extensive investigation of the transformations in question it is not completely clear what is the driving force behind the transformations. Therefore, it is quite possible that the resulting phase assemblies are formed due to kinetic rather than thermodynamic reasons.

5. Reaction densification of α and (α + β) SiAlONs

Densification of SiAlONs occurs by reaction liquid-phase sintering or "transient liquid sintering". Intensive investigations have been done on the reaction liquid-phase sintering of SiAlON in the metal oxide–Si_3N_4–AlN–SiO_2–Al_2O_3 systems.[71–82] Some of the earliest work was carried out in the MgO–Si_3N_4–AlN–SiO_2–Al_2O_3 system.[71–74] It was found that a transient phase, which formed during hot pressing of α-Si_3N_4 with MgO, reacted with α-Si_3N_4 above 1400°C to form β-Si_3N_4 and a vitreous phase.[71] This reaction was found to expedite the sintering kinetics and the reaction pathway of a mixture of MgO–Si_3N_4–AlN–SiO_2–Al_2O_3 depended on the amount of MgO added.[71–73] The addition of Y_2O_3, instead MgO to a Si_3N_4–AlN–SiO_2 mixture resulted in a material with diphasic microstructure consisting of β′-SiAlON and YAG ($Y_3Al_5O_{12}$) with improved mechanical properties.[74] Later the attempts were made to obtain dense β-SiAlON ceramics in the Si_3N_4–AlN–SiO_2–Al_2O_3 system.[75–77] In these studies, it was shown that the sintering kinetics depended on the composition of starting powder mixtures, even though the final composition of the sintered material was the same. In these and other reaction sintering and hot-pressing studies, the densification mechanisms were identified to be solution-reprecipitation,[71–74] fast particle rearrangement,[80] Cobble creep,[80] or grain boundary sliding.[79,81]

Recently, it was shown by Hwang and Chen that reaction hot pressing of α′- and (α + β)-Y-SiAlON took place in three stages.[82] Further, it was found out that the wetting properties of the Y_2O_3–Al_2O_3–SiO_2 eutectic melt controlled the densification behavior of powder compacts. The first stage was identified with the formation of the ternary oxide eutectic and YAG. The shrinkage in this stage was due to the redistribution of liquid in the powder compact and slight improvement in the particle packing densities. The second stage was identified with the wetting of AlN particle and formation of β_{60}. The preferential wetting of AlN by the ternary oxide melt caused localization of the liquid,

leading to a delaying effect on the second shrinkage step. The third stage occurred with the dissolution of αSi_3N_4 and formation of the final phase. Massive particle rearrangement was found to be the dominant densification mechanism. It also caused aluminum enrichment in the liquid, leading to formation of β_{60} as a transient phase. Thus the physical/chemical characteristics of the liquid, in particular its wetting behavior, and the kinetic pathway of the intermediate reactions are clearly important factors in reaction densification of multicomponent systems.

A survey of the literature indicates that until recent time there was very limited knowledge of the wetting characteristics of various ternary oxide eutectic melts on nitrides. Most studies on reaction sintering have been restricted to the documenting of the evolution of phases and densities. Only limited information may be gleaned from the reports of transient/intermediate phases of these studies. The reaction sequence were studied in Ca-, Y- and Nd-α-SiAlON, and, according to Refs. 83 and 84, gehlenite ($Ca_2Al_2SiO_7$) was found to be transient phase in Ca-α-SiAlON, whereas N-melilite ($R_2Si_2O_3N_4$) formed during the densification of Y- and Nd-α-SiAlON. N-melilite was also reported to be a transient phase in Nd- and Sm-doped α-SiAlON.[85,86] The same phase was identified as a transient one during the pressureless sintering of lanthanide (Y and Nd to Lu, except Pm)- modified α-SiAlON.[87] K phase ($RSiO_2N$) and β-Si_3N_4 phase along with melilite were determined in the case of Nd-α-SiAlON in Ref. 38. Furthermore, in the same work J phase ($R_4Si_2O_2N$) and β-Si_3N_4 were reported to occur along with melilite in the case of Sm- and Gd-α-SiAlON, and J phase and β-Si_3N_4 in case of Dy-, Y-, Er- and Yb-α-SiAlON. The reaction sequence in hot-isostatic-pressed and pressureless-sintered, RE-doped (α + β) SiAlONs have been studied.[9,87–90] Formation of 12H and La–Si–oxynitride as the transient phase in the case of Y- or Y/La-doped samples were reported. Generally it has not been known what controls the formation and selection of various phases. The first indication that a general understanding of reaction sequence during sintering of SiAlON materials may, after all, be based on simple physical chemical considerations governing surface activities of nitrides with reactive liquids was given in Ref. 82. There it was shown that in Y-SiAlON system, Y_2O_3–Al_2O_3–SiO_2 melt preferentially wets AlN, leading to the formation of β_{60}-SiAlON as a transient phase, which delays densification in the early stages due to liquid trapping.

A more systematic research of the wetting behavior of ternary eutectic melts Me_2O_3–Al_2O_3–SiO_2 (Me = Li, Mg, Ca, Y, Nd, Sm, Gd, Dy, Er, and Yb) and their influence on the phase development during reaction hot pressing of αSi_3N_4, AlN, Al_2O_3, and Me_2O_3 powder mixtures was accomplished.[91] Later these results were tied in with densification.[92] The evolution of phases on heating was studied by means of heating up the mixtures to some intermediate temperatures, cooling down, and subsequent XRD characterization. The wetting experiments were to study the trends in the wetting behavior of the ternary oxide melts on the nitrides. For this purpose ternary eutectic compositions were prepared and pressed into pellets, which were placed on substrates prepared from Si_3N_4 and AlN by hot pressing without additives. These "sandwiches" were then heated to different temperatures, in a nitrogen atmosphere, where the pellets fused. On cooling, the contact angles were measured from photomicrographs. Since the wetting characteristics are sensitive to the composition (including the oxygen and nitrogen content in the melt) and the temperature, the true equilibrium was not achieved during the experiments.[91] Therefore, these experiments can not be considered as yielding the actual values of the wetting angle.

It was shown that the wetting behavior of the ternary oxide melt towards Si_3N_4 and AlN was strikingly different, depending on the metal oxide used. Such a preference in reaction sequence was explained in terms of acid-base chemistry.[91] According to the Pearson's principle, hard acids preferentially react with soft bases.[47] Empirically, polarizability, electronegativity, and charge to size ratio[47] can be used as a measure of hardness of

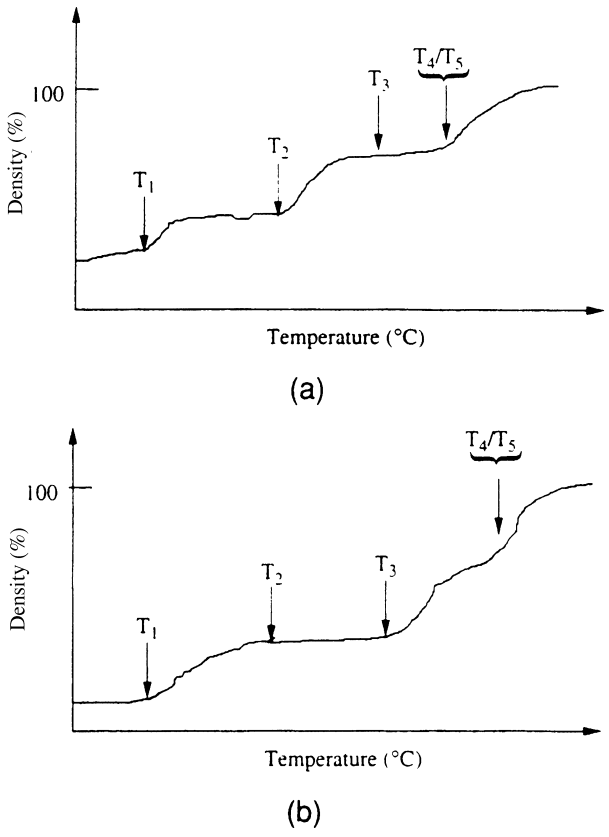

Fig. 22. Schematic shrinkage curves when the eutectic melt wets (a) Si_3N_4, and (b) AlN first.[92]

an acid or a base.[93] Recently, a model of pH_0 (the point of zero charge that corresponds to the pH at which the immersed solid has a zero net surface charge) values calculation for ionic metal oxides based on the ionizational potential of the metal ion was proposed.[94] If the oxides used in Ref. 91 are put in order of decreasing basicity according to this model, and if the acidity of the nitrides is assumed to be determined by the acidity of their native oxide layers (in the case Si_3N_4 will be more acidic than AlN), than both the experimental wetting data and the sequence of the intermediate reaction products in relation to their Si/Al ratio will be in total accordance with the above mentioned acid-base principle. Therefore, the harder acid, Si_3N_4, reacts with hard bases of oxide melts of lithium, calcium, magnesium, and lighter rare earth metals up to gadolinium, whereas the soft acid AlN reacts with the soft bases of the heavier RE metals down to dysprosium. In the order of decreasing Si/Al ratio and additive basicity, typical intermediate phases are O′ (SiN_2O_2), M-cordierite ($Mg_2Al_4Si_5O_{18}$), M′(R) ($R_2Si_2AlO_4N_3$), and β_{60}-SiAlON ($Si_{0.8}Al_{4.2}O_{4.2}N_{3.8}$).

The temperatures for the various reactions, which can be used to understand the shrinkage behavior, were also identified based on the observed wetting and reaction behavior.[87] The reactions identified during the reaction densification of α-SiAlON are:

- the eutectic formation (at temperature T_1),
- wetting of a nitride powder and intermediate phase precipitation (at temperature T_2),
- secondary wetting of the other nitride powder (at temperature T_3),
- dissolution of the intermediate phase (at temperature T_4), and
- precipitation of the final phase, α-SiAlON (at temperature T_5).

Table 8
Summary of features of the shrinkage curves for samples of Me–Si–Al–O–N (Me = Li, Ca, Mg, Nd, Sm, Gd, Dy, Er, Yb) hot pressed at a heating rate of 15°C/min[92]

System	T_1 (°C)	T_2 (°C)	T_3 (°C)	T_4 (°C)	T_5 (°C)	Volume shrinkage	
						First stage	Second stage
Li	1010	1225	1600	1500	1420	8.0	15.0
Ca	1360	1450	1660	1610	1550	5.0	28.0
Mg	1350	1500	1630	>1850	1575	5.0	9.0
Nd	1400	1450	1580	~1800	1420	4.0	15.0
Sm	1380	1460	1600	~1800	1420	7.0	17.0
Gd	1370	1500	1620	1700	1575	7.0	10.0
Dy	1360	~1500	1560	–	1575/1675	5.0	20
Er	1400	~1500	1580	1640	1580	4.0	13.0
Yb	1380	~1500	1560	1640	1560	9.0	10.0

The schematic representation of expected shrinkage curves when the eutectics melt preferentially wets Si_3N_4 and AlN are shown in Fig. 22 (a) and (b), respectively. In these curves, the beginning of various shrinkage steps are identified with some of the above characteristic temperatures. Wetting of AlN is shown to lead to small or no immediate shrinkage in the powder compact because of the low AlN content of the typical SiAlON compact.[82] As it is shown in Fig. 22 (b), though, a subsequent shrinkage step occurs when the majority Si_3N_4 is wetted. Variation of these shrinkage curves may also be possible. For example, it is known that the initial precipitation of the intermediate phase usually starts with partial wetting of the first nitride, i.e., T_2 could be significantly lower than the temperature when complete wetting is achieved. Also, the dissolution of intermediate phase may or may not be higher than T_5. Indeed, T_4 may even be lower than T_3, as in case of lithium and calcium, where wetting and dissolution of the second nitride (AlN) occurs after the intermediate phase (O′) is dissolved and partial formation of α-SiAlON is already achieved.[92] Experimental data on the characteristic temperatures of shrinkage determined for a number of systems are presented in Table 8. Experimental shrinkage curves obtained by means of hot pressing with a constant treating rate[91] were in good agreement with the ones, predicted by the sequence of wetting reactions.

Reaction densification of Me–SiAlON occurs in three stages. The first stage is associated with the formation of the SiO_2–Al_2O_3–Me_2O_3 ternary eutectic (at temperature T_1). The second stage is associated with the preferential wetting of majority nitride powder, Si_3N_4. This occurs at T_2 when Si_3N_4 is wetted first. If AlN is wetted first, then no shrinkage step is observed at T_2 and the densification is delayed until T_3, when Si_3N_4 is wetted finally.

The third stage involves the dissolution of the intermediate phase if T_4 is low; otherwise a distinct third stage is not seen while a gradual densification continues following the second stage. In the extreme case of very high T_4, this may result in poor density as in case of magnesium, where cordierite precipitates as an intermediate phase.

The formation temperature of the final α-SiAlON phase (T_5) is not crucial in most cases, unless a sudden secondary precipitation of α-SiAlON at this later stage (T'_5) drains the liquid and retards densification. Such material must be densified at temperatures below T'_5. To achieve full densification at relatively low temperatures, a low wetting temperature for the second nitride (T_3) and low dissolution temperature of the intermediate phase (T_4) are required. The dominant process for densification in SiAlON ceramics was shown to be massive particle rearrangement although some dissolution facilities full densification by providing the necessary liquid.[92]

More generally, the amount of liquid is controlled by the phase diagram, dissolution of intermediate phase, distribution of liquid and secondary precipitation of α-SiAlON. The effect of viscosity of liquid as opposite to the most of expectations, is relatively insignificant. The different characteristic temperatures that vary widely among the SiAlON systems obscure its effect in most cases. For example, according to Ref. 92, although in heavier RE SiAlONs in isothermal hot pressing the densification time increased slightly in the order of dysprosium, erbium, and ytterbium, most probably due to the influence of viscosity, the densification kinetics in constant heating rate do not reflect the same trend, because of non-monotonic variation of characteristic temperatures.

6. Conclusions

(α + β)–SiAlON composites represent a family of ceramic materials, which are promising from the standpoint of tailoring for specific applications due to the flexibility of their phase composition and microstructure. The latter could be easily modified not only by means of initial composition alterations but rather by means of post-sintering heat treatment. This possibility is provided by the fully reversible α′ to β′ transformation that occurs in the presence of some secondary phases, specifically Al-containing nitrogen melilite solid solutions, M′(R). The mechanism of this transformation is similar to the one occurring in silicon nitride, however in the case of SiAlONs the transformation is not only fully reversible but also may occur in the absence of substantial amounts of intergranular liquid phase since internally-generated liquid phase forms at certain temperatures and under certain conditions. The amount of the latter, although rather small, is sufficient for promoting the reconstructive α′ to β′ transformation.

Stability of phases (α′, M′(R), J′(R), etc.) and of phase assemblages is determined by the RE ionic radius. Therefore, definite properties of (α + β)–SiAlON composites may be achieved by using certain RE as sintering additives.

Sintering behavior of SiAlONs, which can be described as reaction densification in the presence of liquid phase, can be rationalized in terms of simple physicochemical considerations, i.e. of the acid/base reaction principle. Shrinkage and formation of the transient phases during sintering as well as the final phase and microstructure of SiAlON ceramics depends on the preferential wetting of the nitrides by the RE-containing silicate melt.

Overall, the recent findings indicate that a good basis for further SiAlON development has been achieved due to diverse in-depth research of a variety of RE–Si–Al–O–N systems.

Acknowledgements

The financial support of the research activities of Dr. V.A. Izhevskyi by CNPq during his stay at IPEN as an invited scientist are highly appreciated.

References

1. Oyama, Y. and Kamigaito, K., Solid solubility of some oxides in Si_3N_4. *Jpn. J. Appl. Phys*, 1971, **10**, 1637–1642.
2. Jack, K. H., Solid solubility of alumina in silicon nitride. *Trans. J. Brit. Ceram. Soc*., 1973, **72**, 376–378.
3. Jack, K. H. and Wilson, W. I., Ceramics based on the Si–Al–O–N and relates systems. *Nature Phys. Sci. (London)*, 1972, **238**, 28–29.
4. Ekström, T. and Nygren, M., SiAlON ceramics. *J. Am. Ceram. Soc*., 1992, **75**, 259–276.
5. Shelby, J. E. and Kohli, J. T., Rare-earth aluminosilicate glasses. *J. Am. Ceram. Soc*., 1990, **73**, 39–42.
6. Hampshire, S., Drew, R. A. L. and Jack, K. H., Oxynitride glasses. *Phys. and Chem. of Glasses*, 1985, **26**, 82–86.
7. Gauckler, L. J., Lukas, H. L. and Petzow, G., Contribution to the phase diagram Si_3N_4–AlN–Al_2O_3–SiO_2. *J. Am. Ceram. Soc*., 1975, **58**, 346–348.
8. Jack, K. H., The significance of structure and phase equilibria in the development of silicon nitride and sialon ceramics. *Sci. Ceram*, 1981, **11**, 125–142.
9. Ekström, T., Käll, P.-O., Nygren, M. and Olssen, P.-O., Dense single-phase β-sialon ceramics by glass-encapsulated hot isostatic pressing. *J. Mater. Sci*., 1989, **24**, 1853–1861.
10. Huang, Z.-K., Sun, W.-Y. and Yan, D.-S., Phase relations of the Si_3N_4–AlN–CaO system. *J. Mater. Sci. Lett*., 1985, **4**, 255–259.
11. Hampshire, S., Park, H. K., Thompson, D. P. and Jack, K. H., α-Sialon ceramics. *Nature (London)*, 1978, **274**, 880–883.
12. Thompson, D. P., The crystal chemistry of nitrogen ceramics. *Mater. Sci. Forum*, 1989, **47**, 21–42.
13. Mitomo, M., Tanaka, H., Muramatsu, K., Li, N. and Fujii, Y., The strength of α-sialon ceramics. *J. Mater. Sci*., 1980, **15**, 2661.
14. Mitomo, M., Izumi, F., Bando, Y. and Sakikawa, Y., Characterization of α-sialon ceramics. In *Ceramic Components for Engines*, ed. S. Somiya. K.T.K. Science Publishers, Tokyo, Japan, 1984, pp. 377–386.
15. Ishizawa, K., Ayuzawa, N., Shiranita, A., Takai, M., Uchida, N. and Mitomo, M., Some properties of α-sialon ceramics. In *Ceramic Components for Engines*, ed. W. Bunk and H. Hausner. German Ceramic Society, Bad Honnet, Germany, 1986, pp. 511–518.
16. Stutz, D., Greil, P. and Petzow, G., Two-dimensional solid solution forming of Y-containing α- Si_3N_4. *J. Mater. Sci., Lett*., 1986, **5**, 335–336.
17. Huang, Z. K., Tien, T. Y. and Yen, D. S., Subsolidus phase relationship in the Si_3N_4–AlN–rare earth oxide systems. *J. Am. Ceram. Soc*., 1986, **69**, C241–C242.
18. Shen, Z., Nygren, M. and Halenius, U., Absorbtion spectra of rare-earth doped α-sialon ceramics. *J. Mater. Sci. Lett*., 1997, **16**, 263–266.
19. Shen, Z. and Nygren, M., On the extention of the αsialon phase area in yttrium and rare-earth doped systems. *J. Eur. Ceram. Soc*., 1997, **17**, 1639–1645.
20. Mitomo, M., In situ microstructure control in silicon nitride based ceramics. In *Advanced ceramics*, ed. S. Somiya. Elsevier, Barking, Essex, UK, 1988, pp. 147–161.
21. Ekström, T., Effect of composition, phase content and microstructure on the performance of yttrium sialon ceramics. *Mater. Sci. Eng*., 1989, **A109**, 341–349.

22. Fang-Fang, X., Shu-Lin, W., Nordberg, L.-O. and Ekström, T., Nucleation and growth of the elongated α-SiAlON. *J. Eur. Ceram. Soc*., 1997, **17**, 1631–1638.
23. Nordberg, L.-O., Shen, Z., Nygren, M. and Ekström, T., On the extension of the α-SiAlON solid solution range and anisotropic grain growth in Sm-doped α-SiAlON ceramics. *J. Eur. Ceram. Soc*., 1997, **17**, 575–580.
24. Ekström, T., Käll, P.-D., Nygren, M. and Olsson, P. O., Mixed α- and β- (Si–Al–O–N) materials with yttria and neodymia additions. *Mater. Sci. Eng. A105*/, 1988, **106**, 161–165.
25. Mandal, H., Thompson, D. P. and Ekström, T., Reversible α-β SiAlON transformation in heat-treated sialon ceramics. *J. Eur. Ceram. Soc*., 1993, **12**, 421–429.
26. Mandal, H., Thompson, D. P. and Ekström, T., Optimization of sialon ceramics by heat treatment. In *Third Euro-eramics, Vol. 3*, ed. P. Duran and J. F. Fernandez. Faenza Editrice Iberica SL, Spain, 1993, pp. 385–390.
27. Mandal, H., Thompson, D. P., Sun, Y. W. and Ekström, T., Mechanical property control of rare earth oxide densified α- β . In *5th International Symposium on Ceramic Materials and Components for Engines*, ed. D. S. Yan, Y. R. Fu and S. Y. Shi. World Scientific Publishers, Singapore, 1995, pp. 441–446.
28. Mandal, H. and Thompson, D. P., Mechanism of α–β SiAlON transformation. In *Fourth Euro-eramics*, ed. G. Galus Gruppo Editoriale. Faenza Editrice S.p.A, Italy, 1995, pp. 273–280.
29. Cheng, Y.-B. and Thompson, D. P., Aluminum-containing nitrogen melilite phases. *J. Am. Ceram. Soc*., 1994, **77**, 143–148.
30. Camuscu, H., Mandal, H. and Thompson, D. P., Optimized high-temperature sialon ceramics containing melilite as the grain boundary phase. In: *21st Century Ceramics, British Ceramic Proceedings,* Vol. 55, ed. D. P. Thompson. 1996, pp. 239–248.
31. Mandal, H., Cheng, Y.-B. and Thompson, D. P., α-SiAlON ceramics with a crystalline melilite grain-boundary phase. In *Proceedings of the 5th International Symposium on Ceramic Materials and Components for Engines, Shanghai,World Scientific Publishers*, ed. D. S. Yan, Y. R. Fu and S. Y. Shi. Singapore, 1995, 1994, pp. 202–205.
32. Ijevskii, V. A., Kolitsch, U., Seifert, H. J., Wiedmann, I. and Aldinger, F., Aluminum-containing ytterbium nitrogen Woehlerite solid solutions. *Synthesis, Structure and Some Properties. J. Eur. Ceram. Soc*., 1998, **18**, 543–552.
33. Jack, K. H., Fabrication of dense nitrogen ceramics. In *Processing of Crystalline Ceramics, III*, ed. H. Palmour, R. F. Davis and T. M. Hane. Plenum Press, New York, 1978, pp. 561–578.
34. Marchand, R., Jayaweera, A., Verdier, P. and Lang, J., Preparation and characterization of new oxynitrides in the lanthanide–sialon–oxide–nitride system. *Acad. Sci. Paris*, 1976, **C.R. 283**, 675–677.
35. Jack, K. H., Silicon nitride sialons and related ceramics. In *Ceramics and Civilization, Vol. III, High-Technology Ceramics*. American Ceramic Society, Columbus, OH, 1986, pp. 259–288.
36. Wang, P. L., Tu, H. Y., Sun, W. Y., Yan, D. S., Nygren, M. and Ekström, T., Study on the solubility of Al in the melilite systems R_2Si_{3-x} $Al_xO_{3+x}N_{4-x}$ with R = Nd, Sm, Gd, Dy and Y. *J. Eur. Ceram. Soc*., 1995, **15**, 689–695.
37. Harris, R. K., Leach, M. J. and Thompson, D. P., Nitrogen-15 and oxygen-17 NUR spectroscopy of silicates and nitrogen ceramics. *Chem. Mater*., 1992, **4**, 260–267.
38. Wang, P. L., Sun, W. Y. and Yan, D. S., Formation and densification of R-α′-SiAlONs (R = Nd, Sm, Gd, Dy, Er and Yb). In *Silicon Nitride Ceramics: Scientific and Technological Advances,* Vol. 287, ed. I.-W. Chen, P. F. Becher, M. Mitomo, G. Petzow and T.-S. Yen. Materials Research Society, 1993, pp. 387–392.
39. Hoffman, M. J., and Petzow, G., Microstructural design of Si_3N_4 based ceramics. In *Silicon Nitride Ceramics: Scientific and Technological Advances,* Vol. 287, ed. I.-W. Chen, P. F. Becher, M. Mitomo, G. Petzow and T.-S. Yen. Materials Research Society, 1993, pp. 3–14.
40. Chee, K. S., Cheng, Y.-S. and Smith, M. E., The solubility of aluminum in rare earth nitrogen melilite phases. *J. Eur. Ceram. Soc*., 1995, **15**, 1213–1220.
41. Slasor, S., Liddel, K. and Thompson, D. P., The role of Nd_2O_3 as an additive in the formation of α′ and β′ sialons. *Br. Ceram. Proc*, 1086, **37**, 51–64.
42. Käll, P.-O. and Ekström, T., Sialon ceramics made with mixtures of Y_2O_3–Nd_2O_3 as sintering aids. *J. Eur. Ceram. Soc*., 1990, **6**, 119–127.
43. Vainstein, B. K., Fridkin, V. M. and Indenbom, V. L., Crystallochemical radu systems. In *Modern Crystallography II. Structure of Crystals*, ed. B.K. Veinstein, A.A. Chernov and L.A. Shuvalov. Springer, Berlin, Heidelberg, 1982, pp. 78–81.
44. Cao, G. Z. and Metselaar, R., α-Sialon ceramics: a review. *Chem. Mater*., 1991, **3**, 242–253.
45. Huang, Z. K., Liu, S. Y., Rozenflanz, A. and Chen, I. W., Sialon composites containing rare-earth melilite and neighboring phases. *J. Am. Ceram. Soc*., 1996, **79**, 2081–2090.
46. Huang, Z. K. and Chen, I. W., Rare-earth melilite solid solution and its phase relations with neighboring phases. *J. Am. Ceram. Soc*., 1996, **79**, 2091–2097.
47. Huheey, J. E., *Inorganic Chemistry*. Harper and Row, New York, 1983.
48. Huang, Z. K., Yan, D.-S. and Tien, T.-S., Compound formation and melting behavior in the AB compound and rare earth oxide systems. *J. Solid State Chem*., 1990, **85**, 51–55.
49. Chen, I. W. and Thompson, D. P., Preparation and grain boundary devitrification of samarium α-SiAlON ceramics. *J. Eur. Ceram. Soc*., 1994, **14**, 13–21.
50. Huang, Z. K., Greil, P. and Petzow, G., Formation of α-Si_3N_4 solid solution in the system Si_3N_4–AlN–Y_2O_3. *J. Am. Ceram. Soc*., 1983, **66**, C96–C97.
51. Sun, W.-Y., Tien, T.-S. and Yen, T.-S., Solubility limits of α-SiAlON solid solutions in the system Si, Al, Y/N, O. *J. Am. Ceram. Soc*., 1991, **74**, 2547–2550.
52. Sun, W.-Y., Tien, T.-S. and Yen, T.-S., Subsolidus phase relationships in part of the system Si, Al, Y/N, O: the system Si_3N_4–AlN–YN–Al_2O_3–Y_2O_3. *J. Am. Ceram. Soc*., 1991, **74**, 2753–2758.
53. Thompson, D. P., Phase relationship in Y–Si–Al–O–N ceramics. In *Proceedings of the 21st University Conference on Ceramic Science, Tailoring Multiphase and Composite Ceramics*, ed. R. E. Tressler. Plenum Press, New York, 1986, pp. 79–91.
54. Mitomo, M., Izumi, F., Horiuchi, S. and Matsui, Y., Phase relationships in the system Si_3N_4–SiO_2–La_2O_3. *J. Mater. Sci*., 1982, **17**, 2359–2366.
55. Sun, W.Y., Yen, T.-S. and Tien, T.-S., Subsolidus phase relationships in the system RE–Al–O–N (where R = rare earth elements). *J. Solid State Chem*., 1991, **95**, 424–429.
56. Sun, W.-Y., Huang, Z.K., Tien, T.-S. and Yen, T.-S., Phase relationships in the system Y–Al–O–N. *Mater. Sci., Lett*., 1991, **11**, 67–69.
57. Mandal, H., Thompson, D. P. and Ekström, T., Heat treatment of Ln–Si–Al–O–N glasses. In *Proc. 7th. Irish Mater. Forum Conf. IMF7*, ed. M. Buggy and S. Hampshire. Trans. Tech. Publications, Switzerland, 1992, pp. 187–203.
58. Thompson, D. P., New grain-boundary phases for nitrogen ceramics. *Mater. Res. Soc. Symp. Proc*, 1993, **287**, 79–92.
59. Sun, W.-Y., Yan, D.-S., Gao, L., Mandal, H. and Thompson, D. P., Subsolidus phase relationships in the systems Ln_2O_3–Si_3N_4–AlN–Al_2O_3 (Ln = Nd, Sm). *J. Eur. Ceram. Soc*., 1995, **15**, 349–355.
60. Sun, W.-Y., Yan, D.-S., Gao, L., Mandal, H. and Thompson, D. P., Subsolidus phase relationships in the systems Dy_2O_3–Si_3N_4–AlN–Al_2O_3. *J. Eur. Ceram. Soc*., 1996, **16**, 1277–1282.
61. Kolitsch, U., Ijevskii, A., Seifert, H. J., Wiedmann, I. and Aldinger, F., Formation and general characterization of a previously unknown ytterbium silicate (A-type Yb_2SiO_5). *J. Mater. Sci*., 1997, **32**, 6135–6139.

62. Lewis, M. H., Crystallization of grain boundary phases in silicon nitride and SiAlON ceramics. In *Silicon Nitride 93, Key Engineering Materials,* Vols. 89–91, ed. M. J. Hoffmann, P. F. Becker and G. Petzow, Trans. Tech. Pub., 1993, pp. 333–338.
63. Jack, K. H., Review: SiAlONs and related nitrogen ceramics. *J. Mater. Sci*., 1976, **11**, 1135–1158.
64. Hampshire, S., Nitride ceramics. In *Materials Science and Technology, Vol. 11, Structure and Properties of Ceramics*, ed. M. Swain. VCH, Weinheim, 1994, pp. 121–171.
65. Hampshire, S., and Jack, K. H,. The kinetics of densification and phase transformation of nitrogen ceramics. In *Special Ceramics 7,* ed. D. W. Taylor and P. Popper. Proc. Brit. Ceram. Soc., Vol. 31, 1981, pp. 37–49.
66. Shen, Z., Ekström, T. and Nygren, M., Temperature stability of samarium-doped α- SiAlON ceramics. *J. Eur. Ceram. Soc*., 1996, **16**, 43–54.
67. Zhao, R. and Cheng, R. B., Microstructural feature of the α- to β-SiAlON phase transformation. *J. Eur. Ceram. Soc*., 1996, **16**, 529–534.
68. Zhao, R. and Cheng, Y. B., Decomposition of Sm α-SiAlON phases during post-sintering heat treatment. *J. Eur. Ceram. Soc*., 1996, **16**, 1001–1008.
69. Camuscu, H., Thompson, D. P. and Mandal, H., Effect of starting composition, type or rare earth sintering additive and amount of liquid phase on α-β SiAlON transformation. *J. Eur. Ceram. Soc*., 1997, **17**, 599–613.
70. Falk, L. K. L., Shen, Z. J. and Ekström, T., Microstructural stability of duplex α - β SiAlON ceramics. *J. Eur. Ceram. Soc*., 1997, **17**, 1099–1112.
71. Drew, P. and Lewis, M. H., The microstructure of silicon nitride ceramics during hot-pressing transformations. *J. Mater. Sci*., 1974, **9**, 261–269.
72. Lewis, M. H., Powell, B. D., Drew, P., Lumby, R. J., North, B. and Taylor, A. J., The formation of single-phase Si–Al–O–N ceramics. *J. Mater. Sci*., 1977, **12**, 61–74.
73. Lewis, M. H., Bhatti, A. R., Lumby, R. J. and North, B., The microstructure of sintered Si–Al–O–N ceramics. *J. Mater. Sci*., 1980, **15**, 103–113.
74. Lewis, M. H. and Lumby, R. H., Nitrogen ceramics: liquid phase sintering. *Powder Metall*., 1993, **26**, 73–81.
75. Layden, G. K., Process Development for Pressureless Sintering of SiAlON Ceramic Components. Report No. R175-91072-4, United Technologies Research Center, February 1976.
76. Boskovich, S., Gauckler, L. J., Petzow, G. and Tien, T. Y., Reaction sintering forming β-Si_3N_4 solid solution in the system Si, Al/N, OI: sintering of Si_3N_4–AlN mixtures. *Powder Metall. Int*, 1977, **9**, 185–189.
77. Boskovich, S., Gauckler, L. J., Petzow, G. and Tien, T. Y., Reaction sintering forming β-Si_3N_4 solid solution in the system Si, Al/N, OII: sintering of Si_3N_4–SiO_2–AlN mixtures. *Powder Metall. Int*, 1978, **10**, 180–185.
78. Boskovich, S., Gauckler, L. J., Petzow, G. and Tien, T. Y., Reaction sintering forming β-Si_3N_4 solid solution in the system Si, Al/N, O. III: sintering of Si_3N_4–AlN–Al_2O_3 mixtures. *Powder Metall. Int*, 1979, **11**, 169–171.
79. Rahman, M. N., Riley, F. L. and Brook, F. J., Mechanisms of densification during reaction hot-pressing in the system Si–Al–O–N. *J. Am. Ceram. Soc*., 1980, **63**, 648–653.
80. Kuwabara, M., Benn, M. and Riley, F. L., The reaction hot pressing of compositions in the system Al–Si–O–N corresponding to β′-SiAlON. *J. Mater. Sci*., 1980, **15**, 1407–1416.
81. Havier, M. and Hansen, P. L., Hot-pressing and α-β′phase transformation of compositions corresponding to β′-SiAlON. *J. Mater. Sci*., 1990, **25**, 992–996.
82. Hwang, S. L. and Chen, I. W., Reaction hot pressing of α and β;′-SiAlON ceramics. *J. Am. Ceram. Soc*., 1994, **77**, 165–171.
83. Sun, W. Y., Walls, P. A. and Thompson, D. P., Reaction sequences in preparation of Sialon ceramics. In *Non-oxide Technical and Engineering Ceramics Proc. Inter. Conf*., Limerick, Ireland ed. S. Hampshire. Elsevier Applied Science, London, 1986,1985, pp. 105–117.
84. Slasor, S. and Thompson, D. P., Preparation and characterization of Yttrium-α′-SIALONS. In *Non-oxide Technical and Engineering Ceramics Proc. Inter. Conf*., Limerick, Ireland ed. S. Hampshire. Elsevier Applied Science, London, 1986,1985, pp. 223–230.
85. Hampshire, S., O'Reilly, K. P. J., Leigh, J. and Redington, M., Formation of α′-SiAlONs with neodymium and samarium modifying cations. In *High Tech Ceramics*., ed. P. Vincezini. Elsevier Science, Amsterdam, Netherlands, 1987, pp. 933–940.
86. O'Reilly, K. P. J., Redington, M., Hampshire, S. and Leigh, M., Parameters affecting pressureless sintering of α′- SiAlONs with lanthanide modifying cations. In *Silicon Nitride Ceramics Scientific and Technological Advances, Proc. Mat. Res. Soc. Symp*., Vol. **287**, Boston, MA, 30 November–3 December, ed. I. W. Chen, P. F. Mitomo, G. Petzow and T. S. Yen. Materials Research Society, Pittsburgh, 1992, pp. 393–398.
87. Ekström, T. SiAlON ceramics sintered with yttria and rare earth oxides. In *Silicon Nitride Ceramics Scientific and Technological Advances, Proc. Mat. Res. Soc. Symp*., Vol. **287**, Boston, MA, 30 November–3 December, ed. I. W. Chen, P. F. Pedier, M. Mitomo, G. Petzow and T. S. Yen. Materials Research Society, Pittsburgh, 1992, pp. 121–132.
88. Ekström, T. and Olssen, P.-O., β′-SiAlON ceramics prepared at 1770°C by hot-isostatic pressing. *J. Am. Ceram. Soc*., 1989, **72**, 1722–1724.
89. Ekström, T. and Olssen, P.-O., Pressureless sintering of SiAlON ceramics with mixed Y_2O_3–La_2O_3 additions. *J. Mater. Sci., Lett*., 1989, **6**, 119–127.
90. Ekström, T. and Olssen, P.-O., HP- sintered β- and α-β- SiAlONs densified with Y_2O_3 and La_2O_3 additions. *J. Mater. Sci*., 1990, **25**, 1824–1832.
91. Menon, M. and Chen, I. W., Reaction densification of α′-SiAlON. I: wetting behavior and acid-base reactions. *J. Am. Ceram. Soc*., 1995, **78**, 545–552.
92. Menon, M. and Chen, I. W., Reaction densification of α′- SiAlON. II: densification behavior. *J. Am. Ceram. Soc*., 1995, **78**, 553–559.
93. Pearson, R. G., Absolute electronegativity and hardness: application to inorganic chemistry. *Inorg. Chem*., 1988, **27**, 734–740.
94. Carre, A., Roger, F. and Varinot, C., Study of acid/base properties of oxide, oxide glass and glass-ceramic surfaces. *J. Colloid Interface Sci*., 1990, **154**, 174–183.